

AD-A138 938

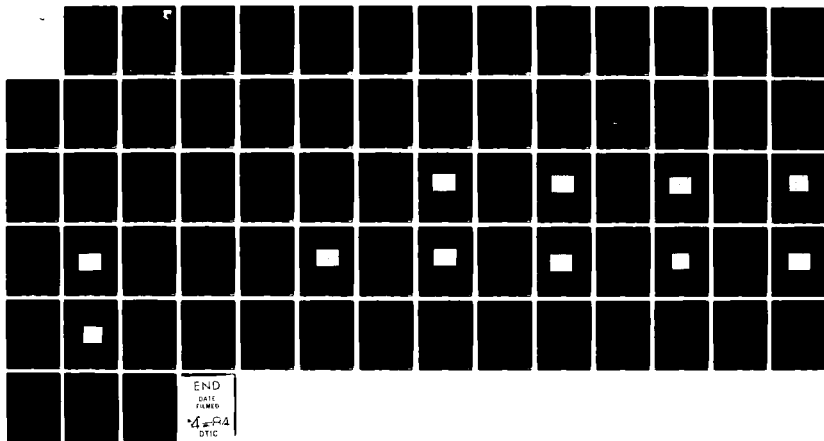
LOW-COST GAAS SOLAR CELL DEVELOPMENT(U) VARIAN
ASSOCIATES INC PALO ALTO CA SOLID STATE LAB
M J LUDOWISE DEC 83 AFWAL-TR-83-2090 F33615-81-C-2025

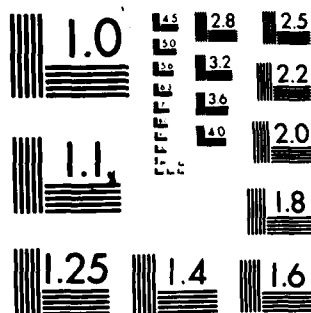
1/1

UNCLASSIFIED

F/G 20/12

NL





MICROCOPY RESOLUTION TEST CHART
NATIONAL BUREAU OF STANDARDS 1963-A

AD A138938

AFWAL-TR-83-2090

LOW-COST GaAs SOLAR CELL DEVELOPMENT

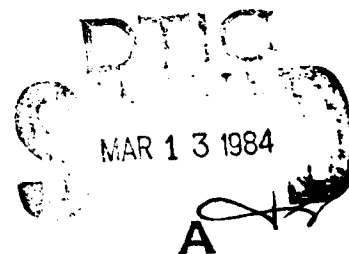
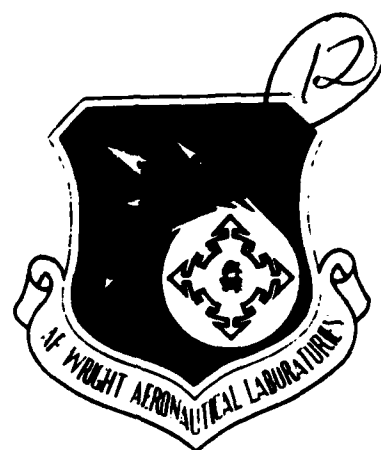
Varian Associates, Inc.
Corporate Solid State Laboratory
611 Hansen Way
Palo Alto, CA 94303

December 1983

Report for Period September 1981 — September 1983

Approved for public release; distribution unlimited.

AERO PROPULSION LABORATORY
AIR FORCE WRIGHT AERONAUTICAL LABORATORIES
AIR FORCE SYSTEMS COMMAND
WRIGHT-PATTERSON AIR FORCE BASE, OHIO 45433



DTIC FILE COPY

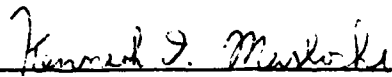
84 03 13 00

NOTICE

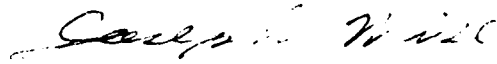
When Government drawings, specifications, or other data are used for any purpose other than in connection with a definitely related Government procurement operation, the United States Government thereby incurs no responsibility nor any obligation whatsoever; and the fact that the government may have formulated, furnished, or in any way supplied the said drawings, specifications, or other data, is not to be regarded by implication or otherwise as in any manner licensing the holder or any other person or corporation, or conveying any rights or permission to manufacture use, or sell any patented invention that may in any way be related thereto.

This report has been reviewed by the Office of Public Affairs (ASD/PA) and is releasable to the National Technical Information Service (NTIS). At NTIS, it will be available to the general public, including foreign nations.

This technical report has been reviewed and is approved for publication.



KENNETH T. MASLOSKI, 2Lt, USAF
Project Engineer
Energy Conversion Branch



JOSEPH F. WISE
TAM, Solar/Thermal Power
Energy Conversion Branch
Aerospace Power Division

FOR THE COMMANDER



JAMES D. REAMS
Chief, Aerospace Power Division
Aero Propulsion Laboratory

"If your address has changed, if you wish to be removed from our mailing list, or if the addressee is no longer employed by your organization please notify AFWAL/POOC-2 W-PAFB, OH 45433 to help us maintain a current mailing list".

Copies of this report should not be returned unless return is required by security considerations, contractual obligations, or notice on a specific document.

UNCLASSIFIED

SECURITY CLASSIFICATION OF THIS PAGE

REPORT DOCUMENTATION PAGE					
1a. REPORT SECURITY CLASSIFICATION Unclassified		1b. RESTRICTIVE MARKINGS			
2a. SECURITY CLASSIFICATION AUTHORITY		3. DISTRIBUTION/AVAILABILITY OF REPORT Approved for public release; distribution unlimited.			
2b. DECLASSIFICATION/DOWNGRADING SCHEDULE					
4. PERFORMING ORGANIZATION REPORT NUMBER(S) AFWAL-TR-83-2090		5. MONITORING ORGANIZATION REPORT NUMBER(S)			
6a. NAME OF PERFORMING ORGANIZATION Varian Associates, Inc.	6b. OFFICE SYMBOL (If applicable)	7a. NAME OF MONITORING ORGANIZATION AFWAL/POOC Wright-Patterson AFB, OH 45433			
6c. ADDRESS (City, State and ZIP Code) 611 Hansen Way Palo Alto, CA 94303		7b. ADDRESS (City, State and ZIP Code) Wright-Patterson AFB, OH 45433			
8a. NAME OF FUNDING/SPONSORING ORGANIZATION	8b. OFFICE SYMBOL (If applicable)	9. PROCUREMENT INSTRUMENT IDENTIFICATION NUMBER F33615-81-C-2025			
8c. ADDRESS (City, State and ZIP Code)		10. SOURCE OF FUNDING NOS.			
		PROGRAM ELEMENT NO.	PROJECT NO.	TASK NO.	WORK UNIT NO.
11. TITLE (Include Security Classification) LOW COST GaAs SOLAR CELL DEVELOPMENT		62203F	3145	19	79
12. PERSONAL AUTHOR(S) Dr. M. J. Ludowise					
13a. TYPE OF REPORT Final	13b. TIME COVERED FROM Sept 81 to Sept 83	14. DATE OF REPORT (Yr., Mo., Day) 1983 December		15. PAGE COUNT 72	
16. SUPPLEMENTARY NOTATION					
17. COSATI CODES			18. SUBJECT TERMS (Continue on reverse if necessary and identify by block number)		
FIELD	GROUP	SUB. GR.			
10	01	02	Gallium Arsenide, solar cells, p/n junction, MOCVD, stop etch thinning.		
20	12				
19. ABSTRACT (Continue on reverse if necessary and identify by block number) An abbreviated program to design and develop a thin, low-cost GaAs solar cell for space applications is described. Due to funding limitations, the scheduled four-year program was terminated at the two-year point. Several growth runs utilizing the metal organic-chemical vapor phase (MO-CVD) epitaxial process were made in an attempt to optimize the solar cell structure. Both p/n and n/p growths were made with varying emitter thickness and doping levels. Cell thinning for selected cells was successful to less than 10 microns using a special stop-etch technique. These cells were covered prior to thinning to provide strength and reduce the probability of breakage.					
20. DISTRIBUTION/AVAILABILITY OF ABSTRACT UNCLASSIFIED/UNLIMITED <input checked="" type="checkbox"/> SAME AS RPT. <input type="checkbox"/> DTIC USERS <input type="checkbox"/>			21. ABSTRACT SECURITY CLASSIFICATION Unclassified		
22a. NAME OF RESPONSIBLE INDIVIDUAL Lt. Ken Masloski			22b. TELEPHONE NUMBER (Include Area Code) 513-255-6235	22c. OFFICE SYMBOL AFWAL/POOC	

DD FORM 1473, 83 APR

EDITION OF 1 JAN 73 IS OBSOLETE.

UNCLASSIFIED
SECURITY CLASSIFICATION OF THIS PAGE

FOREWORD

The work described here was supported by the United States Air Force under the auspices of the Aero Propulsion Laboratory of the Air Force Wright Aeronautical Laboratories at Wright-Patterson Air Force Base under contract F33615-81-C-2025. The program manager was Lt. Kenneth T. Masloski. The program was aimed at designing and building prototype, lightweight, high-efficiency, low-cost GaAs cells in a 2 x 2 cm² format for use at one sun in space.

The work was carried out in the Varian Corporate Research Solid State Laboratory. Dr. P. G. Borden was the principal investigator during the first fifteen months of the program, and Dr. M. J. Ludowise was principal investigator for the remaining seven months. Participating in the work at various stages were Drs. H. C. Hamaker, C. R. Lewis and P. E. Gregory, with the assistance of W. T. Dietze, R. Boettcher, R. A. LaRue and G. Virshup.

The program was originally envisioned as a 40-month program leading to the delivery of fifty 2 x 2 cm² cells. Because of funding gaps and personnel changes, however, the program was terminated at 22 months, including seven months of virtually no funding. This report is a documentation of the final state of the art at 22 MOC, rather than a chronology of development, arranged task by task. It is hoped that this format will prove to be most useful should the development of the devices be resumed some time in the future.



Accession For	
NTIS GRA&I	<input checked="" type="checkbox"/>
DTIC TAB	<input type="checkbox"/>
Unannounced	<input type="checkbox"/>
Justification	<input type="checkbox"/>
By	
Distribution/	
Availability Codes	
Avail and/or	
Special	
A-1	

TABLE OF CONTENTS

SECTION	PAGE
I. OBJECTIVES	1
II. DEVELOPMENT OF FABRICATION TECHNIQUES . . .	2
1. DESIGN OPTIMIZATION -- COMPUTER MODELING	2
a. Description of Model	2
b. Optimization Method	3
c. Results	5
2. GROWTH OF OPTIMIZED STRUCTURES . . .	15
3. GLASS BONDING & CELL THINNING PROCESS .	56
4. OTHER TASKS	59
a. Thin Cell Fabrication	59
b. Welded Contacts	59
c. Cost Study	59
d. Testing	59
e. Cell Deliveries	59
APPENDIX: THINNING PROCESS	60

SUMMARY

An abbreviated program on design and development of a low-cost GaAs/AlGaAs solar cell for space applications is described. A new computer model of the cell was constructed, taking into account experimentally-observed interdependences of parameters (e.g., diffusion length on doping level) and also the flexibility in design offered by the MOCVD epitaxial process. AMO efficiencies between 20 and 21% are predicted, using built-in fields induced by doping gradients.

In parallel with the development of the model, several series of growth runs were made in order to experimentally optimize layer thicknesses and doping levels for maximum efficiency in both p-on-n and n-on-p cells. The desirability of very thin AlGaAs window layers (400 Å) was demonstrated. For p-on-n cells, the optimum emitter thickness lies in the region of 2500 Å, with doping levels of the order of 10^{18} cm^{-3} , and base doping of the order of $2 \times 10^{17} \text{ cm}^{-3}$. Some promising n-on-p growths were made; here the emitter thickness is less critical. Emitter doping of 10^{18} cm^{-3} and base doping of the order of $5 \times 10^{17} \text{ cm}^{-3}$ are close to optimum.

A process was developed for sealing cells to glass cover plates and removing the growth substrate, leaving 6-10 microns of active cell thickness. A detailed description of the process is given.

I. OBJECTIVES

The principal objectives of this work were to demonstrate the fabrication of high-efficiency, lightweight, AlGaAs/GaAs solar cells for use at 1 AMO sun insolation. The epitaxial technique of choice was MOCVD, which allows a high degree of control in the design of the individual cell layers. Two major fabrication areas have been addressed:

1. improved MOCVD techniques, to overcome limitations in cell structure and performance previously associated with LPE processes, and
2. the technology of thinning the cell.

The program saw the development of a technique for growing void-free MOCVD layers, and subsequently the development of techniques for bonding to glass and thinning to the epitaxial layer. Viable designs for the contact metallizations were also worked out.

The work was divided into two major subtasks: 1) development of fabrication techniques and 2) testing. The first task contained several subtasks including design optimization, growth of optimized structures, glass bonding technology, thinning techniques, thin cell fabrication, welded contacts, and cost studies. The final status of each of these will be described in detail in the following sections.

II. DEVELOPMENT OF FABRICATION TECHNIQUES

The overall thrust of Task 1 was to develop the design of, and fabrication techniques for the manufacture of, $2 \times 2 \text{ cm}^2$ cells. The key components of the various subtasks are the MOCVD growth of high-quality epitaxial layers, bonding the wafers to glass and thinning to the epitaxial layers, and contacting the resulting structure. The material quality had to produce high internal quantum efficiency structures, cells with high open circuit voltage (V_{oc}) under 1 AMO sun illumination, and structures free of defects (voids) which can cause shorting of the thinned cell upon metallization. Another key component was the development of a computer model of these cells. The model was to define theoretical upper limits, design optimized cells, analyze subminimal cells, and guide the overall progress of the program.

The following is a breakdown of the final status of each subtask.

1. DESIGN OPTIMIZATION: COMPUTER MODELING

The computer program "SPAOPT2" calculates the performance values of a single-junction, AMO AlGaAs/GaAs solar cell. The program has the capability of optimizing the values of the various physical parameters of the solar cell (i.e., doping levels, layer thicknesses, etc.) in order to obtain the highest efficiency possible. The final version of "SPAOPT2" optimizes thirteen variables, as will be described below, and preliminary runs of the program have yielded theoretical efficiencies in excess of 20% AMO.

a. Description of the Model

The cell design includes a n/p or p/n homojunction with an $\text{Al}_x\text{Ga}_{1-x}\text{As}$ window and an anti-reflection (AR) coating deposited on the

window. The doping levels within the base and emitter regions can be either a linear or an exponential function of the distance from the junction, thereby creating electric fields to enhance minority carrier collection and hence improve the spectral response and inhibit the injected dark current. A standard pattern of narrow parallel gridlines is included on the top side of the cell.

Table 1 lists the key variables of the program. They are listed under one of three categories: optimizable, user input parameters, or calculated. Also included in the program are the AMO spectral data and material properties of GaAs, including absorption coefficient vs photon wavelength, the mobility and diffusion length vs doping levels, and the intrinsic carrier density.

For calculating cell performance, the procedure begins by determining the transmission coefficient through the AR coating and the AlGaAs window as a function of wavelength. The depletion region characteristics and spectral response are then calculated, followed by the spectral response of the emitter and base regions. For the latter, the continuity and current equations must be solved with the doping levels, mobilities, diffusion lengths, and electric fields being functions of position. This is done by subdividing each region into 400 lamella, and solving the equations in reduced matrix form. The injected dark current characteristics are obtained using similar equations, while the Sah-Noyce-Shockley expression is used for the recombination dark current; the tunneling dark current is assumed to be negligible. The final step of the calculation determines the I-V characteristics.

b. Optimization Method

"SPAOPT 2" employs a two-step optimization scheme, first using the gradient-search technique to approach the set of parameter values

TABLE 1: "SPAOPT2" VARIABLES

<u>Optimizable Parameters</u>	<u>User Input Parameters</u>	<u>Calculated Values</u>
Emitter thickness	Emitter recombination velocity	Efficiency
Base thickness	Base recombination velocity	Open-circuit voltage
Emitter doping at surface	Temperature	Short-circuit current
Emitter doping at junction	Gridline resistivity	Fill factor
Base doping at surface	Contact resistance	Internal spectral response
Base doping at junction	Cell Area	
Index of refraction (AR coating)	Cell aspect ratio	
Concentration of Al in window	Emitter type (n or p)	
AR thickness	Grading type (linear or exponential)	
Window thickness		
Gridline spacing	Solar concentration	
Gridline width	Diffusion length damage coefficient	
Gridline aspect ratio	Radiation fluence	

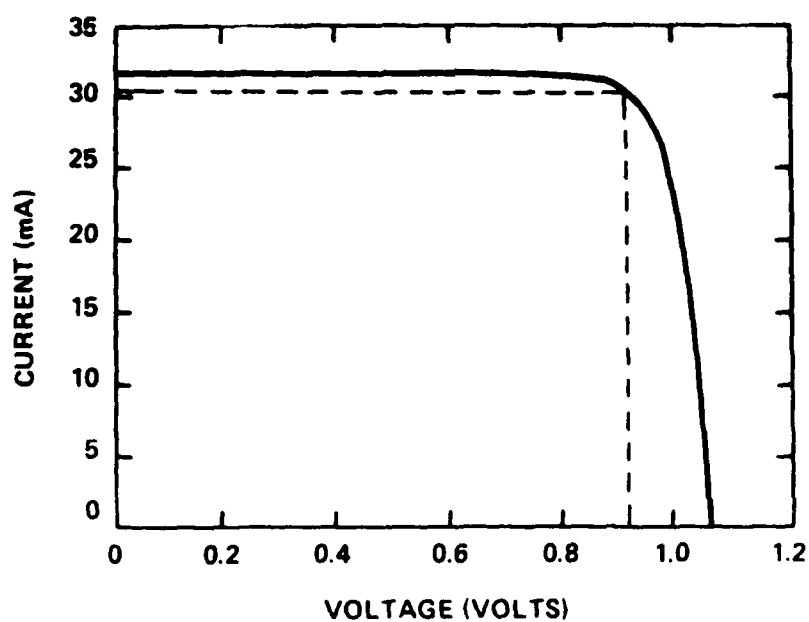
giving the maximum efficiency and second using the parabolic expansion method. The former algorithm causes the search to proceed along the path of steepest ascent from the initial point, whereas the latter method approximates the functional dependence of the efficiency near its maximum as a quadratic of the parameters. This two-step approach has been chosen because the gradient search is most effective away from the maximum, whereas the parabolic expansion is most effective at the maximum.

Since the path of the search proceeds towards the nearest local maximum, the choice of the initial values of the parameters is critical. Thus, various sets of "optimal" values may be obtained from successive runs. It is therefore desirable that a wide range of initial values be tried to locate the global maximum.

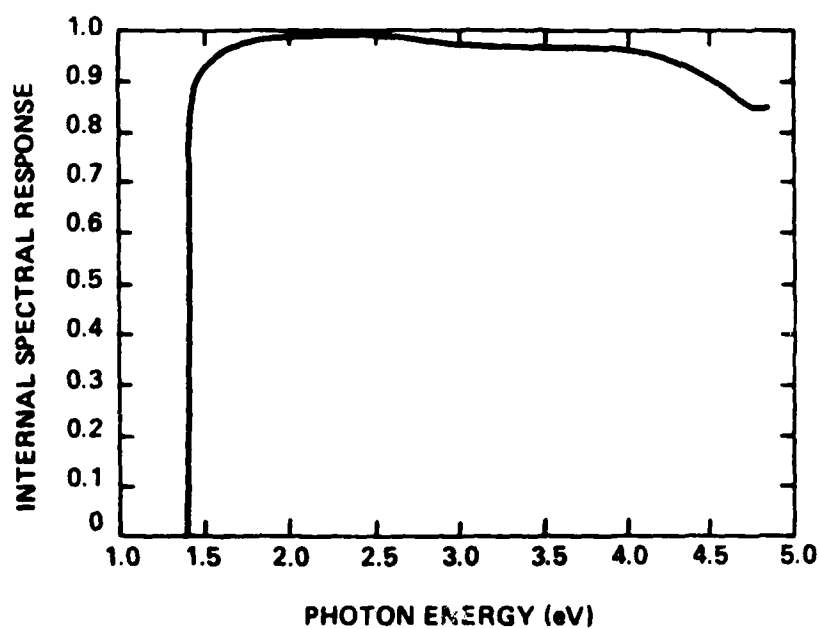
c. Results

Figures 1 to 3 show the results of two runs of "SPAOPT2" which have different sets of the initial values of the optimizing variables, which are indicated by an asterisk. The second run produced a somewhat higher efficiency than the others, thereby illustrating the existence of multiple local maxima, as discussed in the previous section. Even with this limited sampling, we are able to draw some conclusions.

First, the creation of electric fields within the base and emitter through graded doping drastically improves the spectral response. Even with comparatively modest fields (~ 500 V/cm in the emitter, ~ 300 V/cm in the base), we observe high spectral response up to 5 eV. Second, the emitter thickness should be small ($\sim 0.5 \mu\text{m}$), as expected due to the high absorption coefficient of GaAs and the low mobility of the holes in the n-type emitter. Third, the Al fraction of the window should be as high as possible in order to minimize the absorption by this layer; in practice, x will probably be fixed at about 0.8 because of the diffi-



(a)



(b)

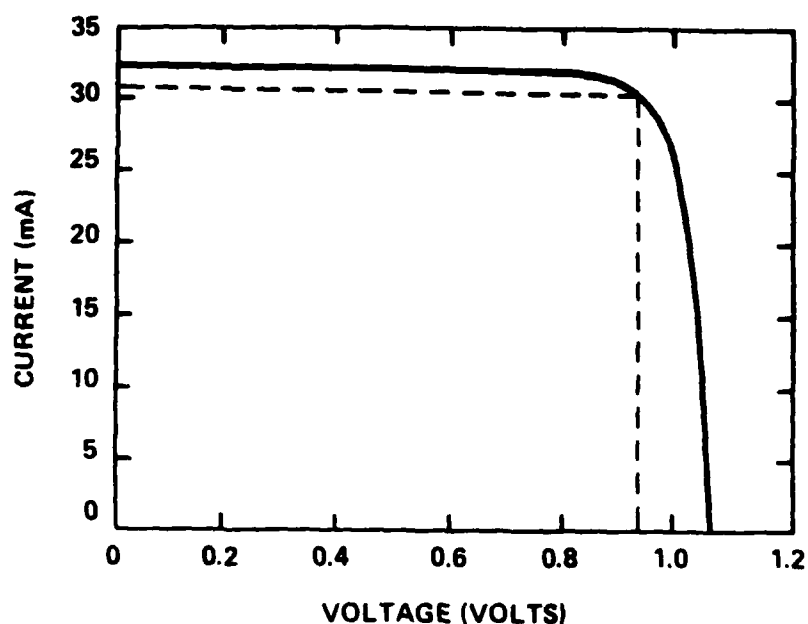
Fig. 1 Calculated current-voltage and spectral response curves using the "SPAOPT2" model for a GaAs n-on-p space cell. The overall projected efficiency is 20.5%.

Fig. 1(a) Efficiency = 20.4593908802
Open Circuit Voltage = 1.0601457661 volts
Short Circuit Current = 0.0315323131487 amperes
Fill Factor = 0.828073872871
Maximum Power = 0.0276815558609 watts
Voltage at Maximum Power = 0.913525183614 volts
Current at Maximum Power = 0.0303019077715 amperes

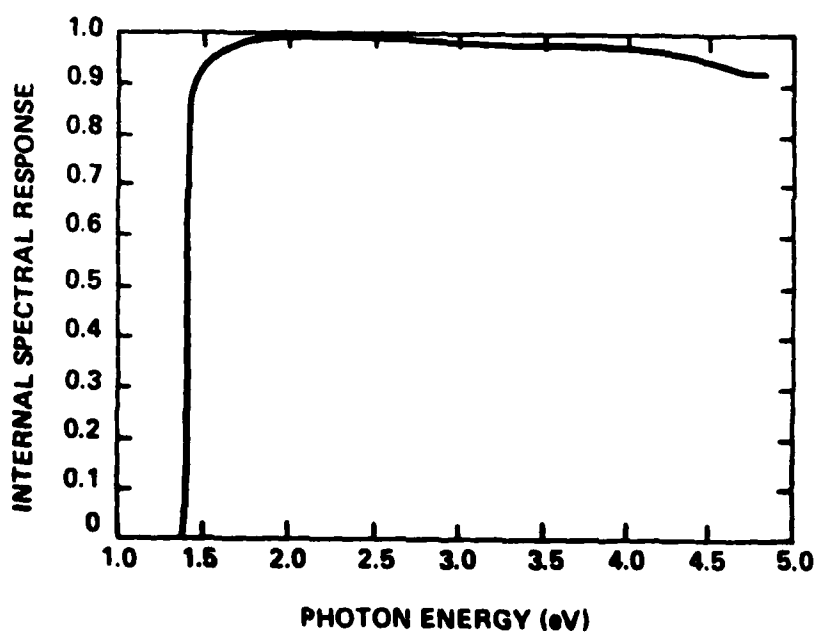
Fig. 1(b) Efficiency = 0
Fill Factor = 0.828073872871
Short Circuit Current = 0.0315323131487
Open Circuit Voltage = 1.0601457661
No. of Emitter Points = 100
No. of Base Points = 100
Emitter Thickness = 0.632 microns

* BASE THICKNESS = 3.675 microns	0.000
* EMITTER DOPING AT SURFACE = $3.66\text{E}+18/\text{cm}^3$	0.00E+00
* EMITTER DOPING AT JUNCTION = $9.23\text{E}+17/\text{cm}^3$	0.00E+00
* BASE DOPING AT JUNCTION = $4.88\text{E}+17/\text{cm}^3$	0.00E+00
* BASE DOPING AT SUBSTRATE = $1.11\text{E}+18/\text{cm}^3$	0.00E+00
FRONT RECOMBINATION VELOCITY = $1.00\text{E}+04$ cm/sec	
BACK RECOMBINATION VELOCITY = $1.00\text{E}+06$ cm/sec	
* INDEX OF A.R. COATING = 1.342	0.000
* THICKNESS OF A.R. COATING = .090 microns	0.000
* ALUMINUM FRACTION OF WINDOW = .992	0.000
* THICKNESS OF WINDOW = .039 microns	0.000
DIFF. LENGTH DAMAGE COEFF. = $1.00\text{E}-08$	
FLUENCE = $5.00\text{E}+16/\text{cm}^2$	
SOLAR CONCENTRATION = 1	
CELL AREA = 1 cm^2	
CELL ASPECT RATIO = 1	
* GRIDLINE SPACING = 200.0 microns	
* GRIDLINE WIDTH = 5.006 microns	
* GRIDLINE ASPECT RATIO = .125	
# OF EMITTER ELEMENTS = 75	
# OF GRIDLINE ELEMENTS = 25	
EMITTER IS N-TYPE	
GRADING IS L	
RADIATION EFFECTS INCLUDED? -N	
A.R. COATING OMITTED? -N	
IV-PLOT DESIRED? -Y	
DAY: 0 TIME: 00:06:49	

Fig. 1 Legend



(a)



(b)

Fig. 2 Calculated current-voltage and spectral response curves using the "SPAOPT2" model for a GaAs n-on-p space cell. The overall projected efficiency is 21.1%. Note the thinner emitter, thicker base, lower emitter doping, steeper base gradient doping, and lower Al fraction in the window, relative to the cell of Fig. 1.

Fig. 2(a)

Efficiency	=	21.1350081691
Open Circuit Voltage	=	1.0556596802 volts
Short Circuit Current	=	0.0320683172018 amperes
Fill Factor	=	0.84469536557
Maximum Power	=	0.0285956660528 watts
Voltage at Maximum Power	=	0.92624880968 volts
Current at Maximum Power	=	0.0308725536313 amperes

Fig. 2(b)

No. of Emitter Points	=	100	
No. of Base Points	=	100	
Emitter Thickness	=	0.476 microns	.100
Base Thickness	=	4.554 microns	.300
Emitter Doping at Surface	=	$1.17\text{E}+18/\text{cm}^3$	$5.00\text{E}+17$
Emitter Doping at Junction	=	$6.25\text{E}+17/\text{cm}^3$	$1.00\text{E}+17$
Base Doping at Junction	=	$2.98\text{E}+17/\text{cm}^3$	$1.25\text{E}+16$

*	BASE DOPING AT SUBSTRATE = $2.00\text{E}+18/\text{cm}^3$	1.00E+17
	FRONT RECOMBINATION VELOCITY = $1.00\text{E}+04$ cm/sec	
	BACK RECOMBINATION VELOCITY = $1.00\text{E}+06$ cm/sec	
*	INDEX OF A.R. COATING = 0.074 microns	.020
*	THICKNESS OF A.R. COATING = 1.517	.010
*	ALUMINUM FRACTION OF WINDOW = 0.971	.050
*	THICKNESS OF WINDOW = 0.031 microns	.005
	DIFF. LENGTH DAMAGE COEFF. = $1.00\text{E}-08$	
	FLUENCE = $5.00\text{E}+16/\text{cm}^2$	
	SOLAR CONCENTRATION = 1	
	CELL AREA = 1 cm^2	
*	GRIDLINE SPACING = 220.5 microns	2.50
*	GRIDLINE WIDTH = 6.978 microns	.100
*	GRIDLINE ASPECT RATIO = 0.297	.020
	NO. OF EMITTER ELEMENTS = 75	
	NO. OF GRIDLINE ELEMENTS = 25	
	EMITTER IS N-TYPE	
	GRADING IS L	
	RADIATION EFFECTS INCLUDED? -N	
	A.R. COATING OMITTED? -N	
	IV-PLOT DESIRED? -Y	

DAY: 0

TIME: 08:42:36

Fig. 2 Legend

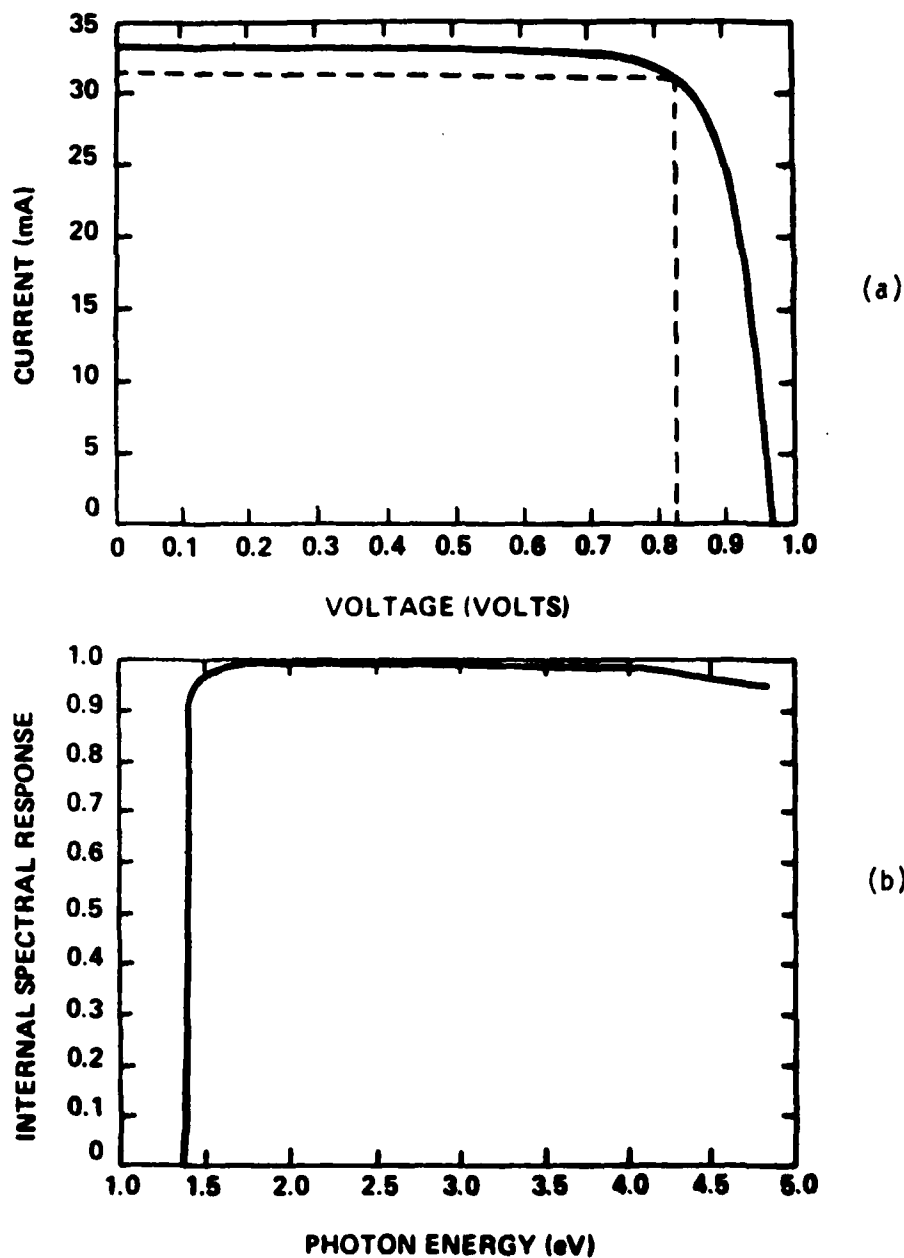


Fig. 3 Calculated current-voltage and spectral response curves using the "SPAOPT2" model for a GaAs n-on-p space cell. The overall projected efficiency is 19.3%. Note the thicker base, lower base and emitter dopings, and thinner window, relative to the cell of Fig. 1.

Fig. 3(a)

SECOND ITERATION #1

Efficiency = 19.2820400174

Open Circuit Voltage = 0.971033784977 volts

Short Circuit Current = 0.032970124654 amperes

Fill Factor = 0.814884105403

Maximum Power = 0.0260886001435 watts

Voltage at Maximum Power = 0.827900195884 volts

Current at Maximum Power = 0.0315117695022 amperes

Fig. 3(b)

No. of Emitter Points = 100

No. of Base Points = 100

Emitter Thickness = 0.628 microns .100

Base Thickness = 5.085 microns .300

Emitter Doping at Surface = $1.03\text{E}+17/\text{cm}^3$ $1.00\text{E}+16$

Emitter Doping at Junction = $1.13\text{E}+16/\text{cm}^3$ $1.00\text{E}+15$

* BASE DOPING AT JUNCTION = $1.10\text{E}+16/\text{cm}^3$	1.00E+15
* BASE DOPING AT SUBSTRATE = $1.06\text{E}+17/\text{cm}^3$	1.00E+16
FRONT RECOMBINATION VELOCITY = $1.00\text{E}+04$ cm/sec	
BACK RECOMBINATION VELOCITY = $100\text{E}+06$ cm/sec	
* INDEX OF A.R. COATING = 1.472	.050
* THICKNESS OF A.R. COATING = 0.082 microns	.010
* ALUMINUM FRACTION OF WINDOW = 0.996	.050
* THICKNESS OF WINDOW = 0.032 microns	.010
DIFF. LENGTH DAMAGE COEFF. = $1.00\text{E}-08$	
FLUENCE = $5.00\text{E}+16/\text{cm}^2$	
SOLAR CONCENTRATION = 1	
CELL AREA = 1 cm^2	
CELL ASPECT RATIO = 1	
* GRIDLINE SPACING = 284.0 microns	20.00
* GRIDLINE WIDTH = 7.159 microns	.100
* GRIDLINE ASPECT RATIO = 0.123	.020
NO. OF EMITTER ELEMENTS = 75	
NO. OF GRIDLINE ELEMENTS = 25	
EMITTER IS N-TYPE	
GRADING IS L	
RADIATION EFFECTS INCLUDED? -N	
A.R. COATING OMITTED? -N	
IV-PILOT DESIRED? -Y	

DAY: 0 TIME: 23:34:06

Fig. 3 Legend

culties in processing AlAs. It is also possible that a thin protective layer of $\text{Al}_{0.8}\text{Ga}_{0.2}\text{As}$ on top of a pure AlAs may be desirable.

A high doping level is also useful. Comparing the third run with the others, the low efficiency primarily results from the relatively low open-circuit voltage, which in turn is determined, to a first approximation, by the built-in voltage V_{bi} . Since $V_{bi} = kT/ne \ln(N_D N_A / n_i^2)$, where N_D , N_A and n_i are the donor, acceptor, and intrinsic concentration densities at the junction, respectively, then the low doping levels account for the observed effects. The good spectral response of Fig. 2 indicates, however, that the poorer mobilities and diffusion lengths of the electrons and holes at high doping levels is not a restrictive factor in cell performance.

The results quoted in this section came towards the end of the program, and hence were not available to guide the growth portion of the work.

2. GROWTH OF OPTIMIZED STRUCTURES

Several variations of the basic cell structure were proposed. These included graded doping in the base layer (graded base), graded windows, minority carrier barriers in the base (back surface fields), and various thicknesses of the window emitter and variations of emitter doping.

Three distinct series of growths were made to compare and evaluate the variations. The spectral response of the wafer was used as the primary evaluation and V_{oc} of selected cells as the secondary criteria. The spectral responses proved to be the most useful.

The first series consists of eight growths. Three design considerations learned from early work were used:

1. The window boundary, if one is used at all, should only be graded down from about 10% AlGaAs in a short distance, in order to avoid excess absorption in the grading layer.
2. Doping grading in the base should be done in the first micron from the junction to be effective.
3. A BSF should be located near the junction, within 1-1.5 microns to be effective.

Table 2 shows the growth run numbers and the features incorporated in each.

TABLE 2: WAFER GROWTHS

<u>Identifier</u>	<u>Graded Window Boundary</u>	<u>Graded Base</u>	<u>Back Surface Field</u>
30M315	X	X	X
30M316		X	X
30M317		X	
30M318	X	X	
30M319	X		X
30M320	X		
30M321			X
30M322			

These wafers were contacted and their spectral response measured using a monochromator. Figure 4 shows the response of all wafers except 30M318. The contact to 30M318 were poor. The axes are photon energy on the horizontal and electrons per absorbed photon (EPAP) on the vertical. For reference, cell 30M318 #2 is also plotted. This had a 20% AlGaAs layer buried 2 μ m into the base, and is close to the ideal performance.

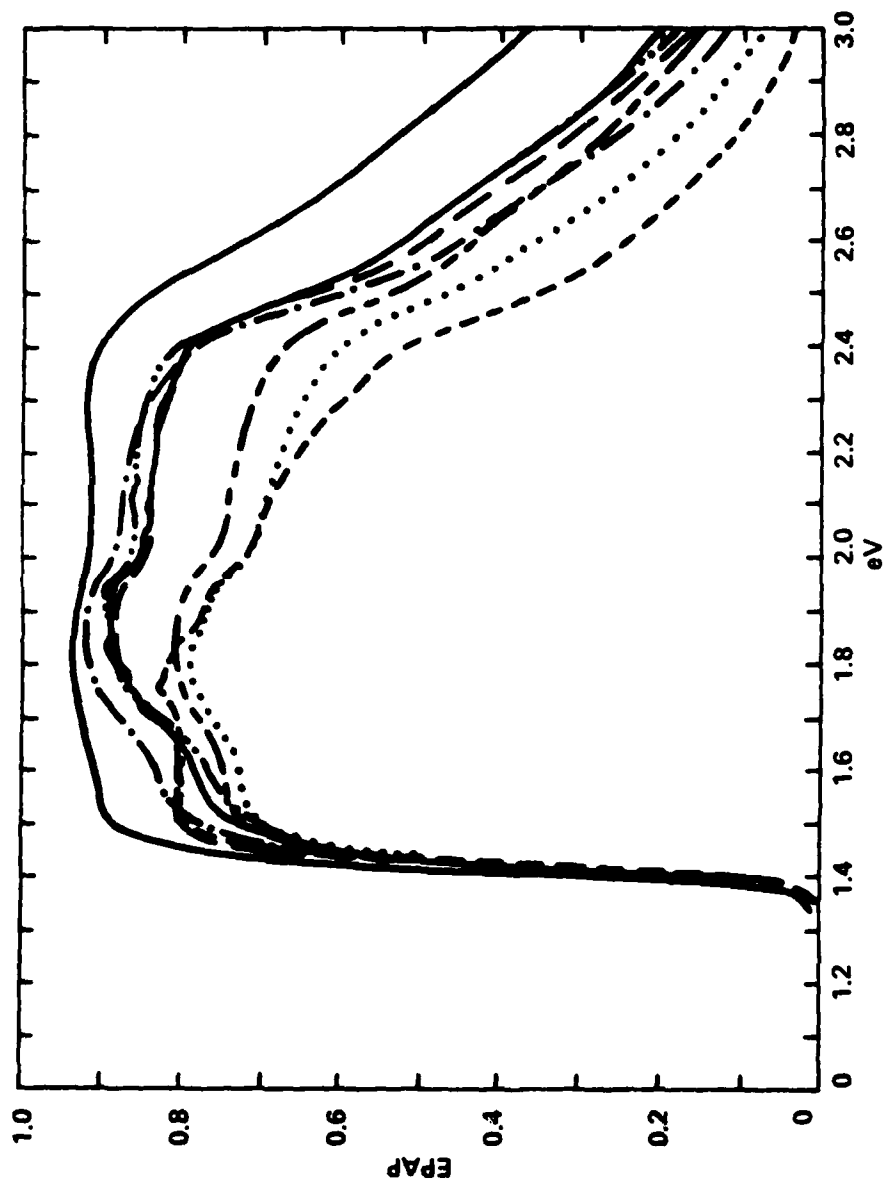


Fig. 4 Spectral response of a series of early GaAs p-on-n cell growths (30M-315 through -322), incorporating graded window boundaries, graded bases and back surface field.

The spectral response curves are shown separately in Figs. 5 to 11, with 30M318 omitted. The important features of the responses are tabulated in Table 3. In general, several valuable observations and conclusions can be drawn from the data.

TABLE 3: GROWTHS OF p-on-n CELLS

<u>Growth</u>	<u>Emitter (all doped $2 \times 10^{18} \text{cm}^{-3}$)</u> <u>Thickness ($\text{\AA}$)</u>	<u>Base Doping</u>
Lost in Process	1000	$4 \times 10^{17} \text{cm}^{-3}$
30M372	1000	1×10^{18}
30M388	2000	4×10^{17}
30M371	2000	1×10^{18}
30M373	3000	4×10^{17}
30M370	3000	1×10^{18}

First, cells with graded window boundaries performed worse than identical cells with the graded windows omitted. This can be seen by direct comparison of 30M315 and 30M316, or 30M319 with 30M321. Second, the graded base improves response somewhat in conjunction with the back surface field, but does not appear to enhance the red response as much as expected. Third, the back surface field does not change response significantly beyond expected run-to-run variations. The valuable result from these runs is that the thinnest possible window, without grading at the window boundary, produces the most desirable response.

Another series of growths was made to evaluate optimum emitter thickness in both n and p cells and study quantum yield as a function of base doping. The p/n cells will be treated first. Table III shows the relevant parameters of the six wafers examined. Two base dopings, 4×10^{17} and $1 \times 10^{18} \text{cm}^{-3}$, and three emitter thicknesses, 1000, 2000, and

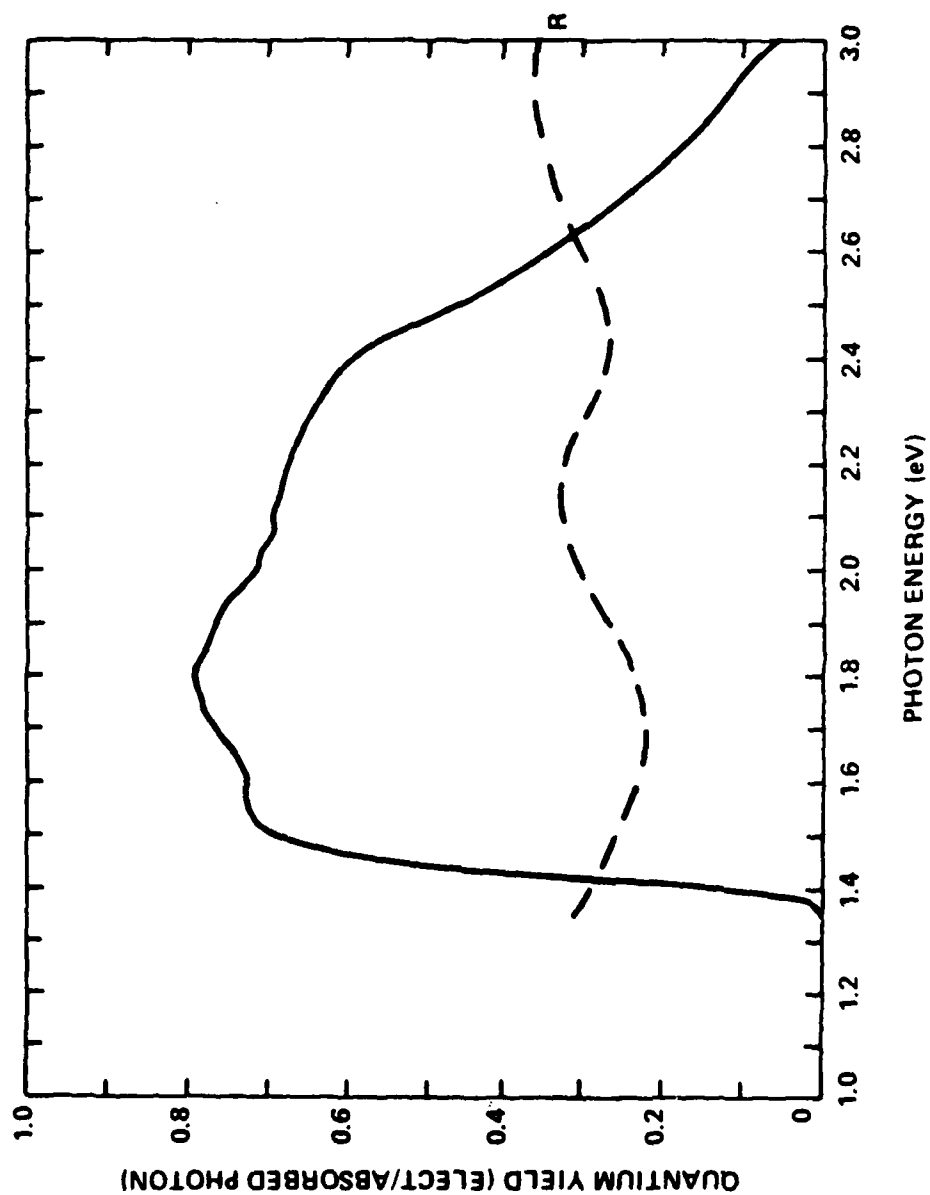


Fig. 5 Spectral response curve of GaAs cell 30M-315, containing a graded window boundary, graded base and a back surface field.

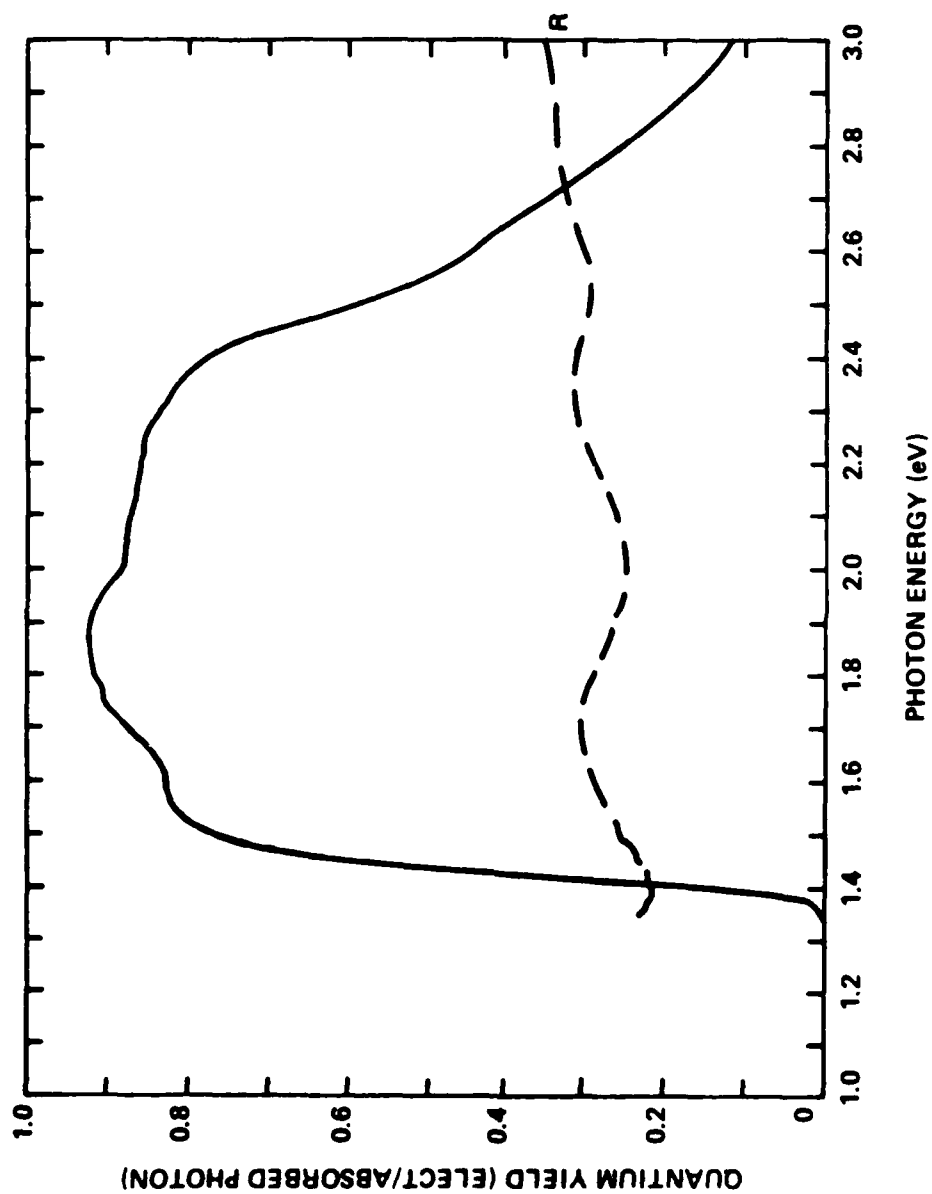


Fig. 6 Spectral response curve of GaAs cell 30M-316, containing a graded base and a back surface field.

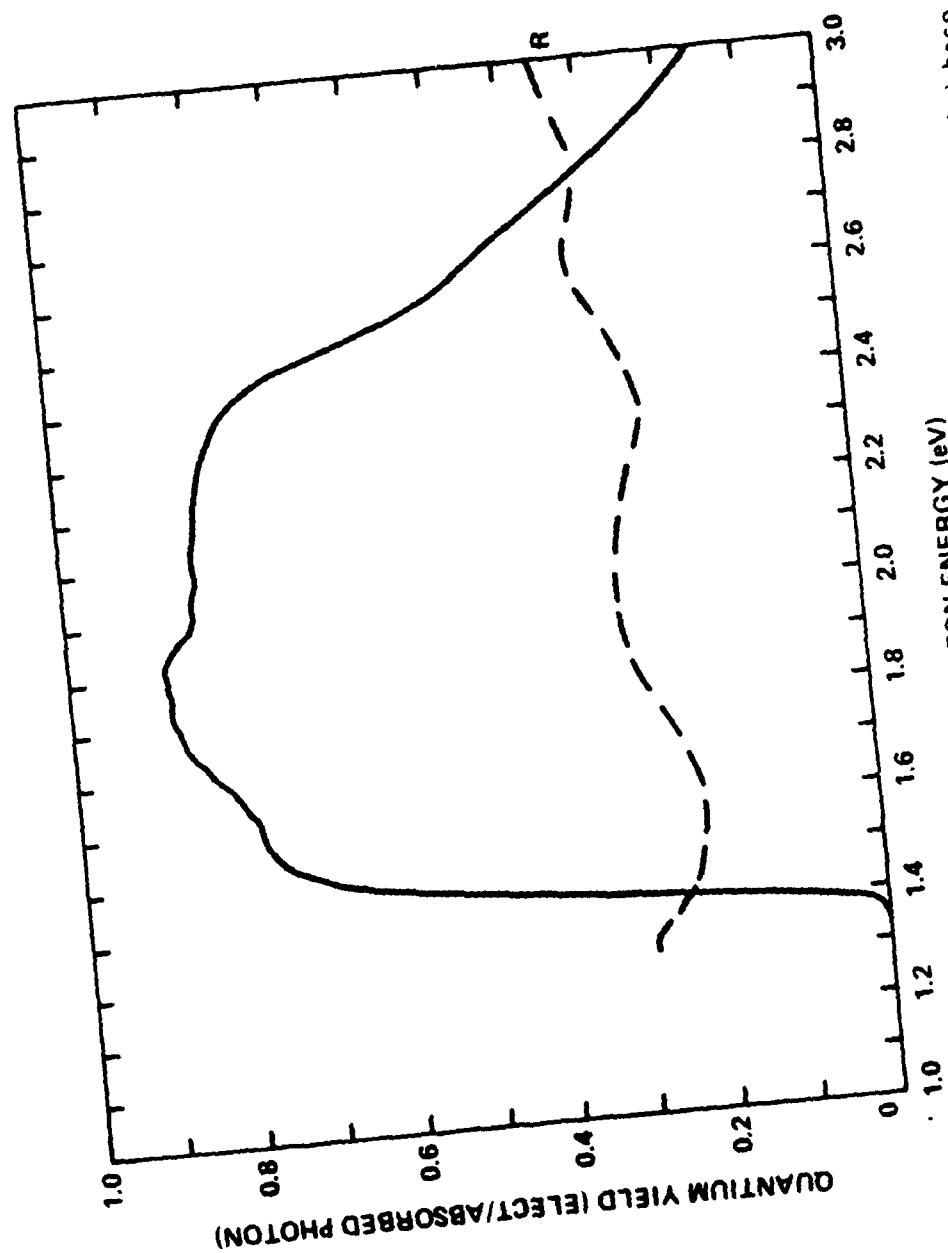


Fig. 7 Spectral response curve of GaAs cell 30M-317, containing a graded base.

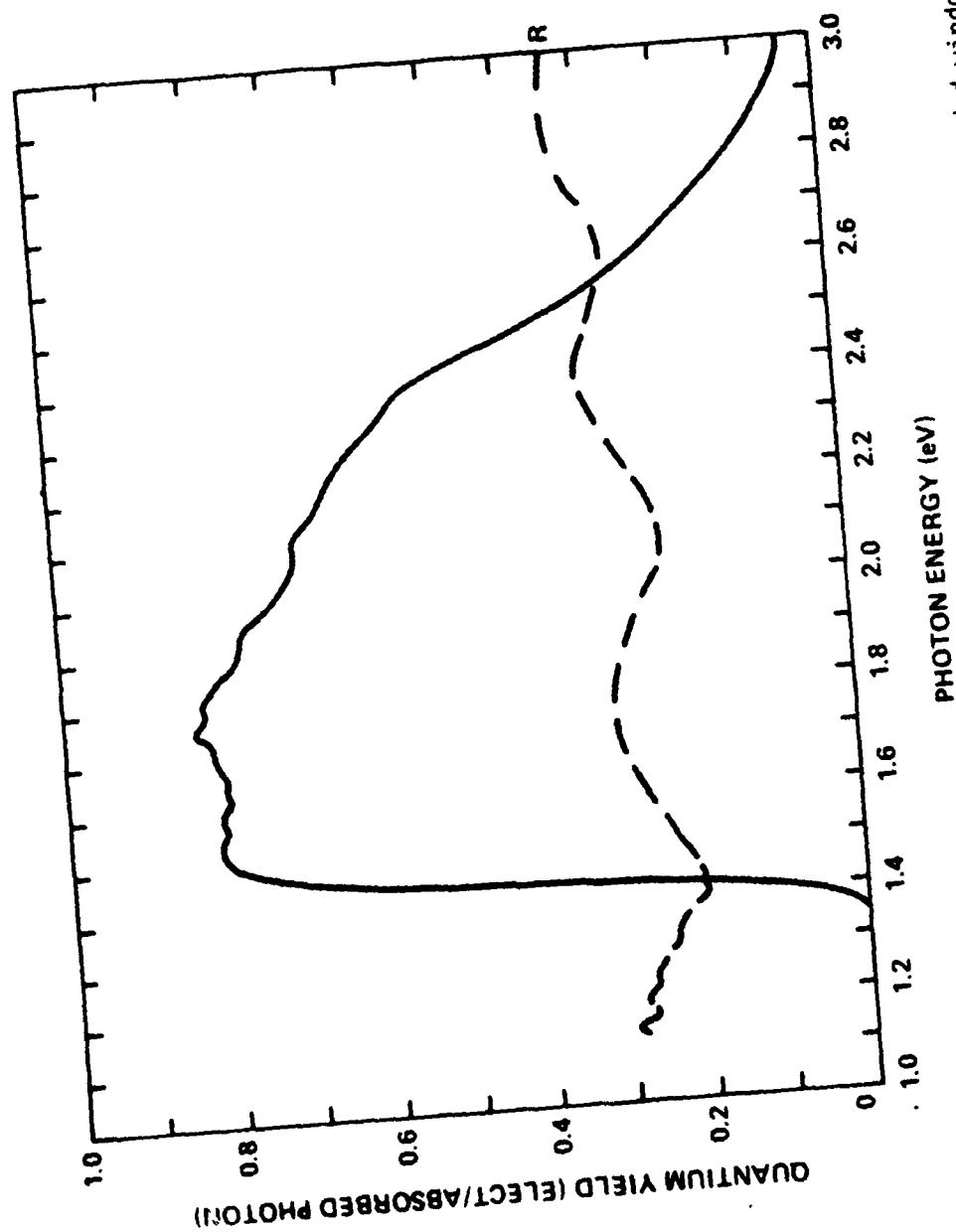


Fig. 8 Spectral response curve of GaAs cell 30M-319, containing a graded window boundary and back surface field.

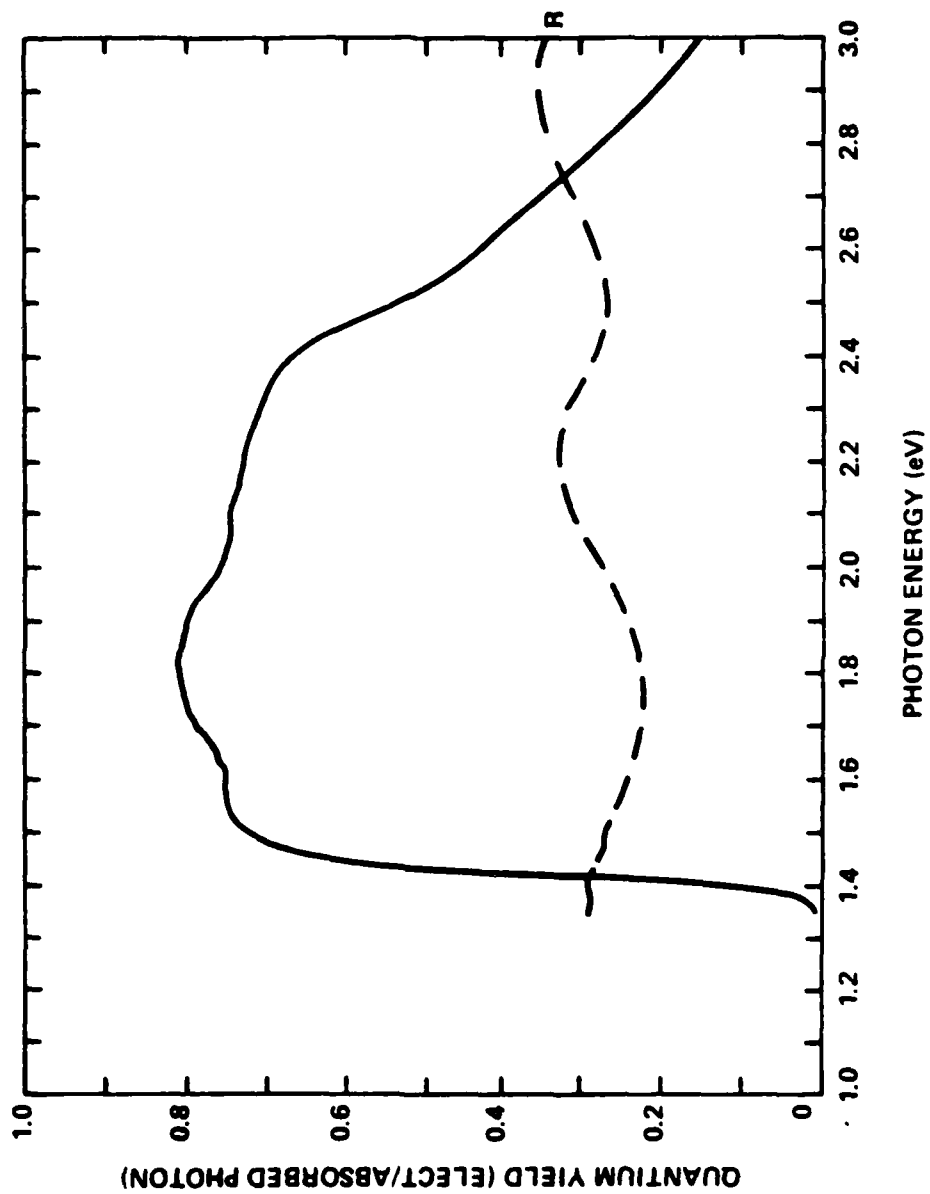


Fig. 9 Spectral response curve of GaAs cell 30M-320, containing a graded window boundary.

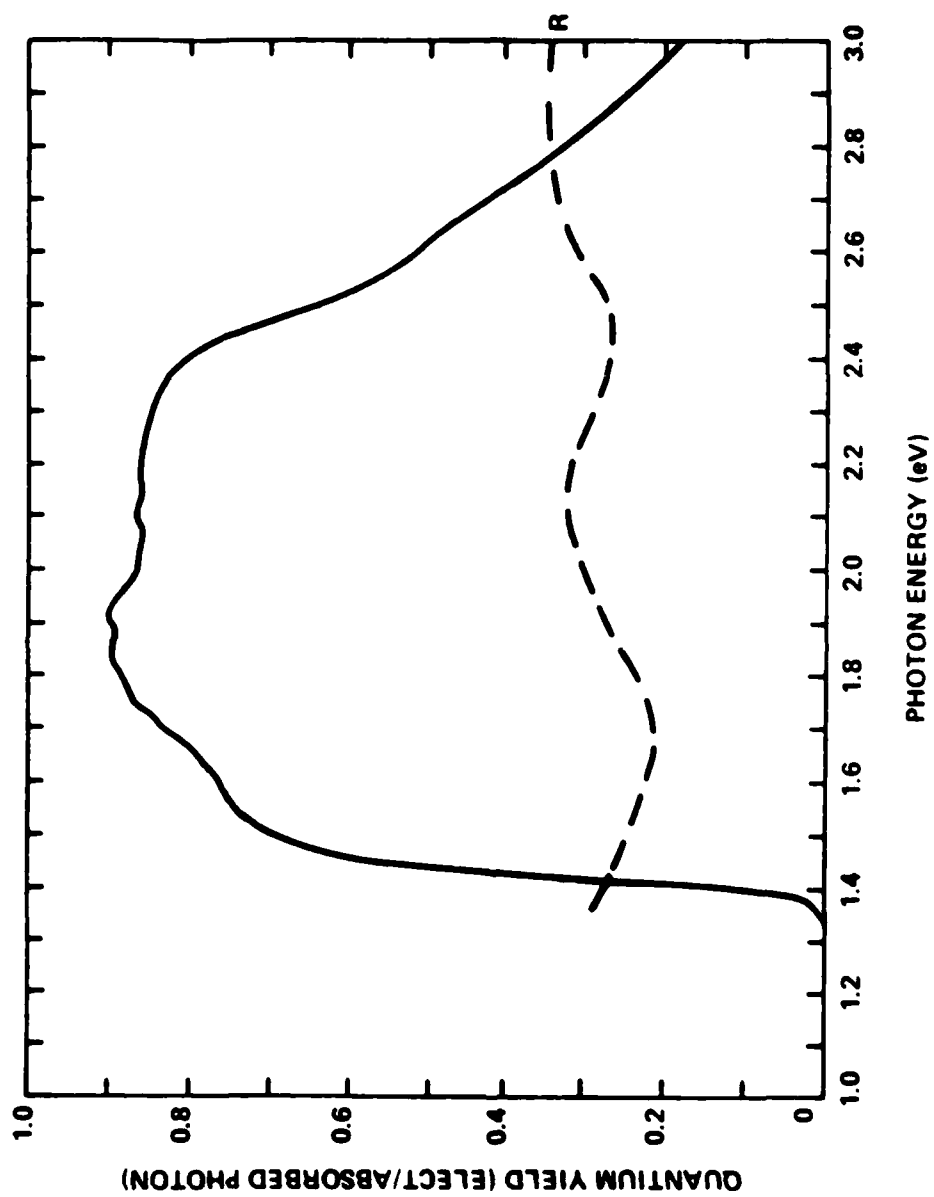


Fig. 10 Spectral response curve of GaAs cell 30M-321, containing a back surface field.

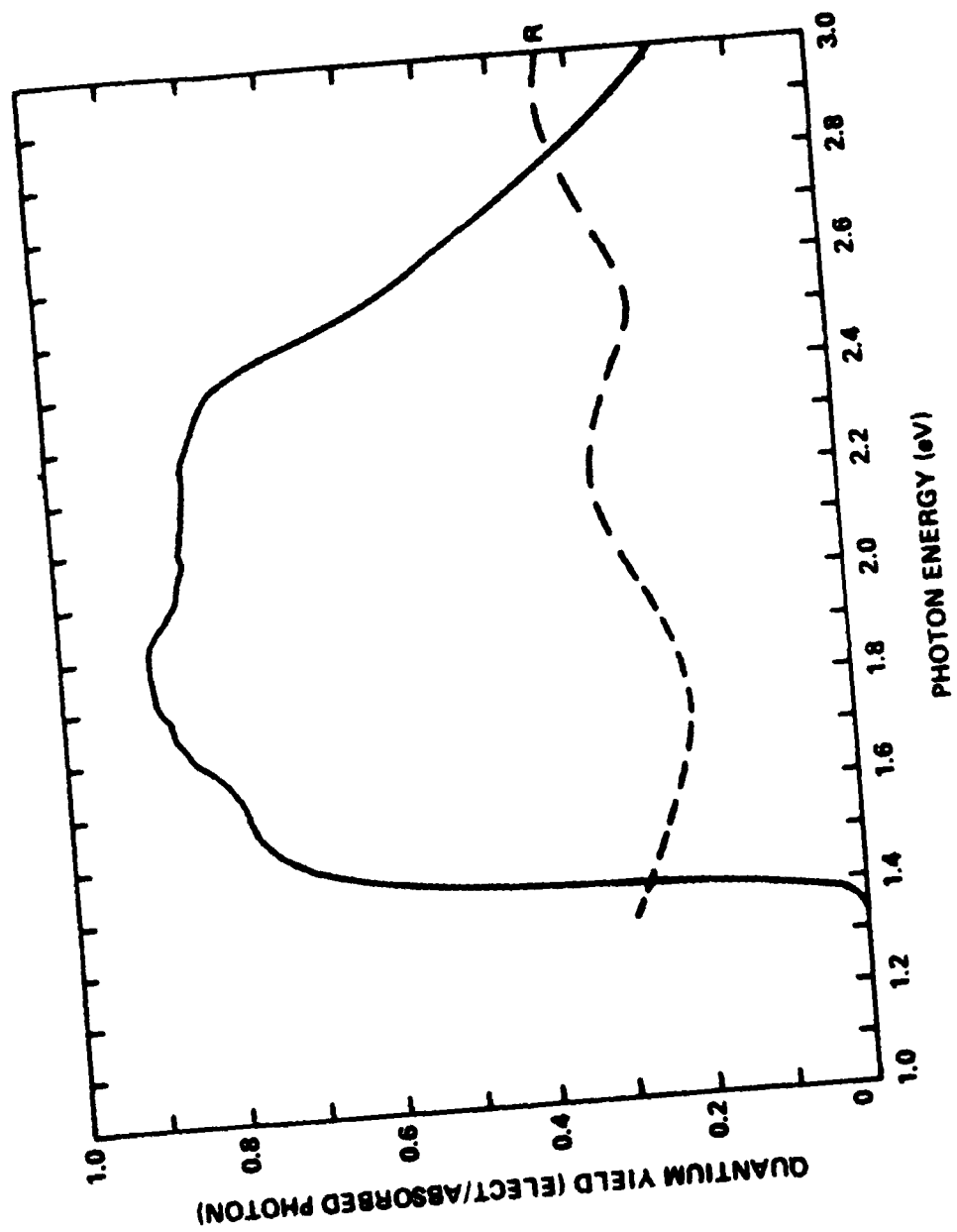


Fig. 11 Spectral response curve of GaAs control cell 30M-322.

3000 Å were examined. The 2000 Å thickness is believed to be ideal from a radiation hardness standpoint, and was chosen as the midpoint. The remaining parameters are: a 2-μm base, constant emitter doping of $p = 2 \times 10^{18} \text{ cm}^{-3}$, a 1500 Å $\text{Al}_{0.90}\text{Ga}_{0.10}\text{As}$ window layer and a two-layer cap with the lower layer 0.3-μm thick, doped $p = 2 \times 10^{18} \text{ cm}^{-3}$ and the upper layer 0.2-μm thick, doped $p = 6 \times 10^{18} \text{ cm}^{-3}$. This structure assists in lowering grid contact resistance.

Figures 12 to 16 display the spectral response and I-V curves of fully fabricated cells (11% obscuration) made from these wafers. (The first wafer, the 1000 Å emitter with the $4 \times 10^{17} \text{ cm}^{-3}$ doped base, was lost in processing.) For the three $1 \times 10^{19} \text{ cm}^{-3}$ doped base samples, the spectral response curves differ very little, within experimental error. There is only an inconsequential shift in the red response corresponding to slightly enhanced base carrier collection. The red response is enhanced when the base doping is lowered to $n = 4 \times 10^{17} \text{ cm}^{-3}$, because of higher L_p .

The blue response is nearly constant on all the samples, suggesting that L_n (diffusion length of electrons in the emitter) is much larger than 3000 Å maximum emitter thickness. Data from n-on-p cells indicates L_n is higher than 2 μm.

Figure 17 shows the average and range of the open circuit voltage (V_{oc}) and short circuit current (I_{sc}) from cells proposed with these wafers. As expected, the higher base doping yields a higher open circuit voltage, but lower short circuit current. The former is due to the higher doping difference across the junction; the latter is due to the poorer red response. It appears, however, that the improvement in V_{oc} is small compared to the price paid in I_{sc} . This is because $1 \times 10^{18} \text{ cm}^{-3}$ doping is degenerate, so that the shift in Fermi level is small for the amount of extra dopant added. It thus appears desirable to use lower base dopings.

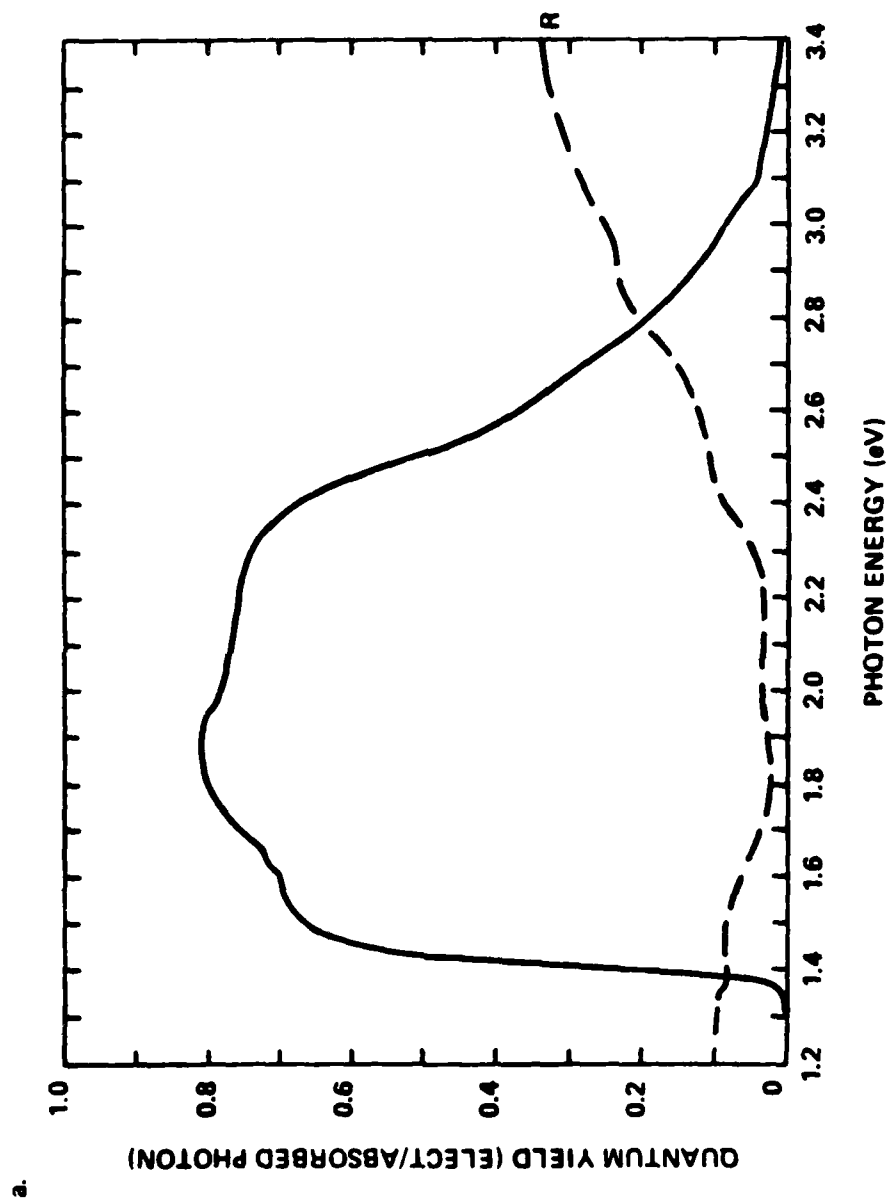


Fig. 12a Spectral response curve of GaAs p-on-n cell (30M-372) with a 1000 Å thick emitter and a base doping of $1 \times 10^{18} \text{ cm}^{-3}$.

B.

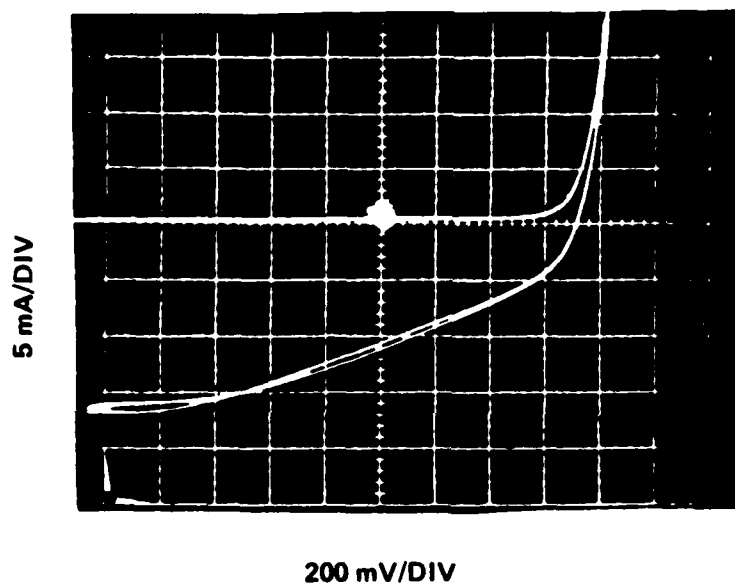


Fig. 12b I-V characteristics (in dark and under illumination of the cell in Fig. 12a.

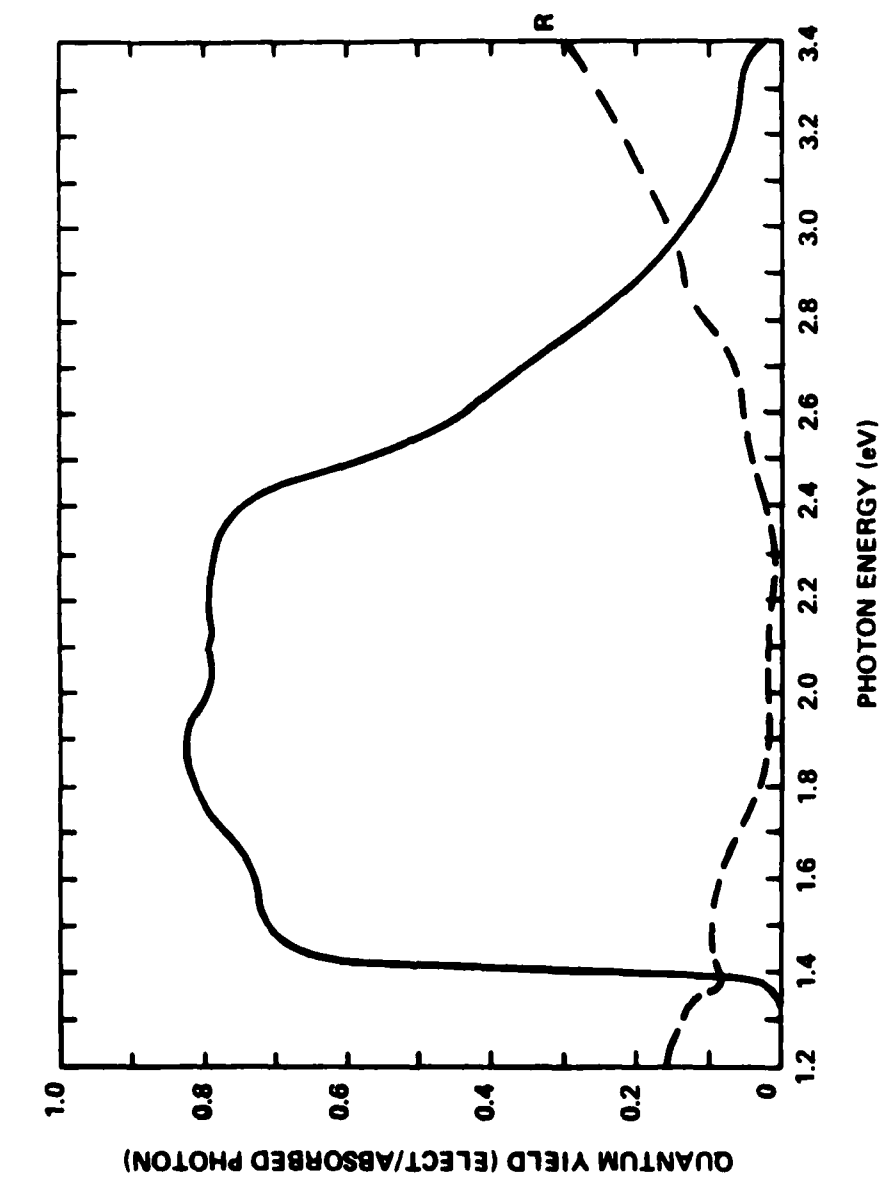


Fig. 13a Spectral response curve of a GaAs p-on-n cell (30M-388) with a 1000 Å thick emitter and a base doping of $4 \times 10^{17} \text{ cm}^{-3}$.

B.

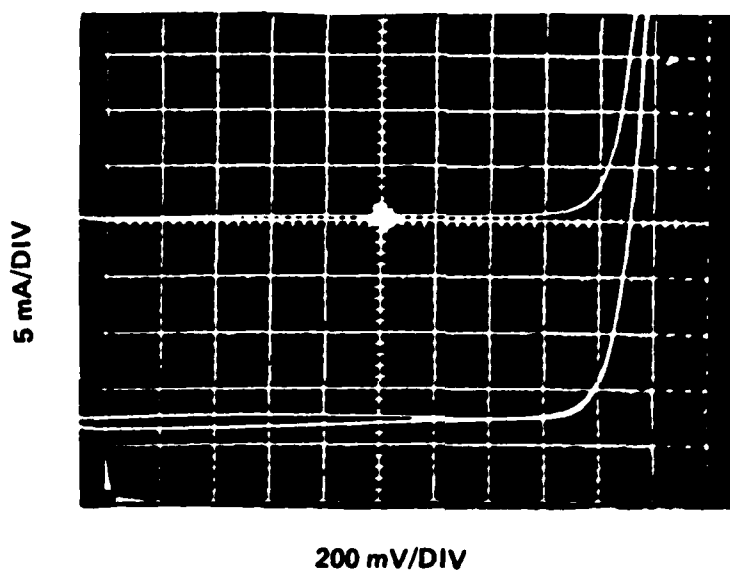


Fig. 13b. I-V characteristics (in dark and under illumination) of the cell in Fig. 13a.

a.

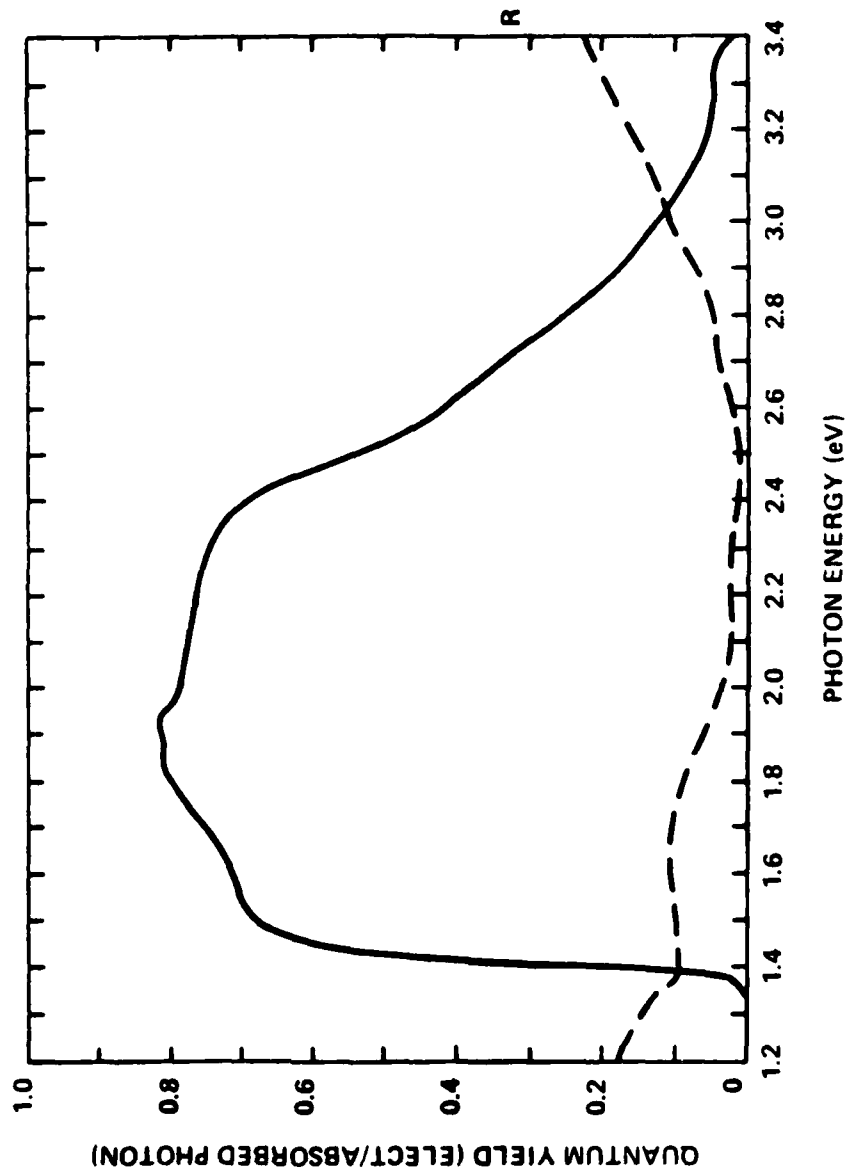


Fig. 14a. Spectral response curve of a GaAs p-on-n cell (30M-371) with a 2000 Å thick emitter and a base doping of $1 \times 10^{18} \text{ cm}^{-3}$.

B.

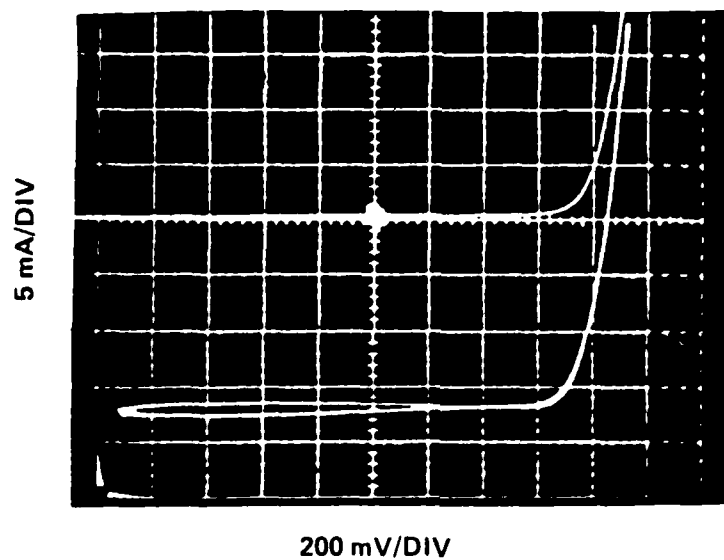


Fig. 14b. I-V characteristics (in dark and under illumination) of the cell in Fig. 14a.

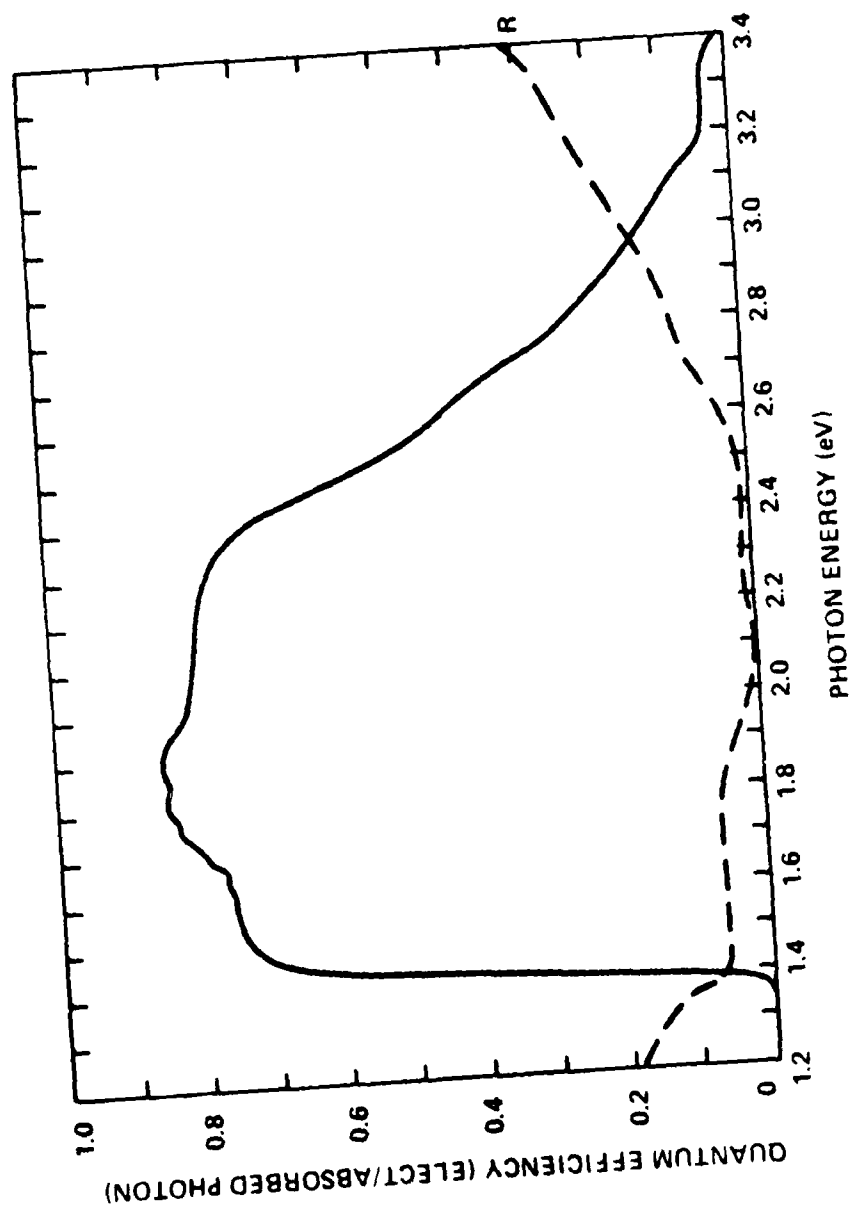


Fig. 15a. Spectral response curve of a GaAs p-on-n cell (30M-373) with a 3000 Å thick emitter and a base doping of $4 \times 10^{17} \text{ cm}^{-3}$.

B.

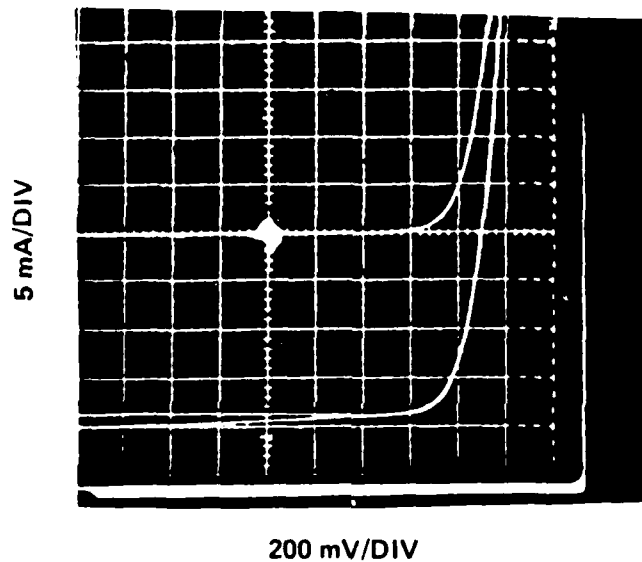


Fig. 15b. I-V characteristics (in dark and under illumination) of the cell in Fig. 15a.

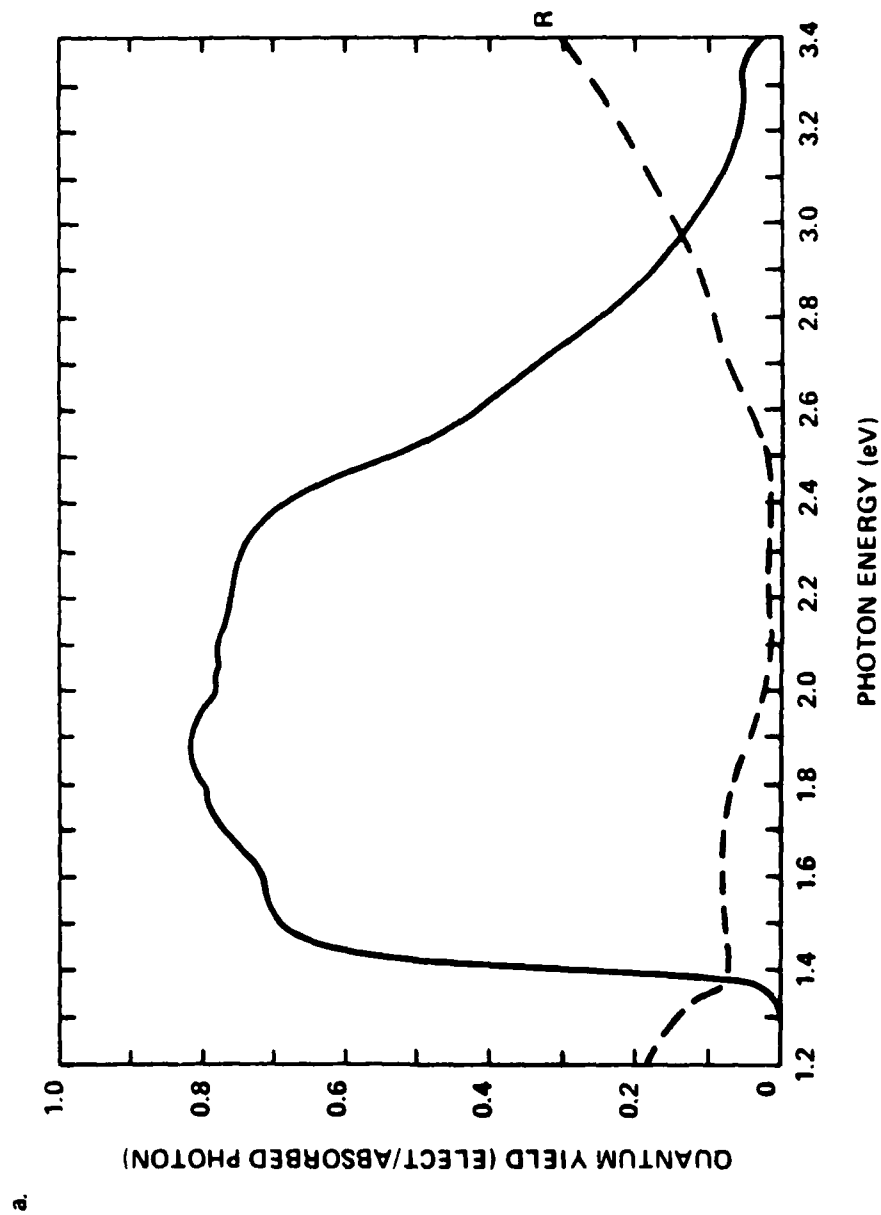


Fig. 16a. Spectral response curve of a GaAs p-on-n cell (30M-370) with 3000 Å thick emitter and a base doping of $1 \times 10^{18} \text{ cm}^{-3}$.

B.

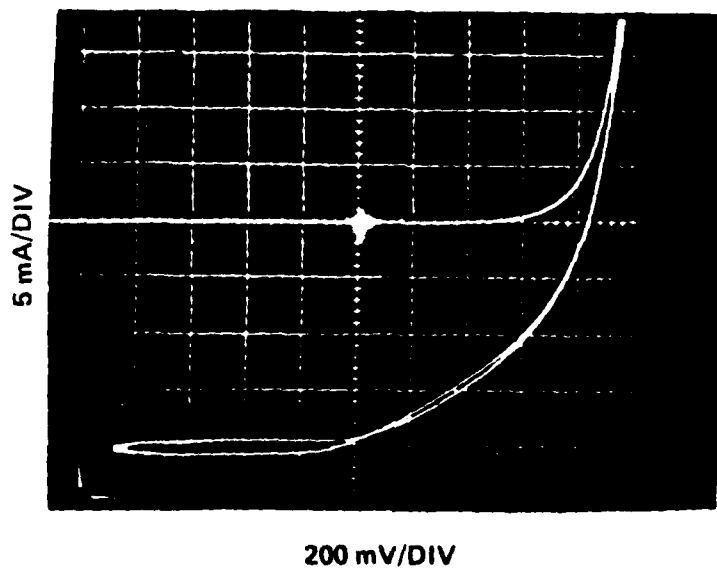


Fig. 16b. I-V characteristics (in dark and under illumination) of the cell in Fig. 16a.

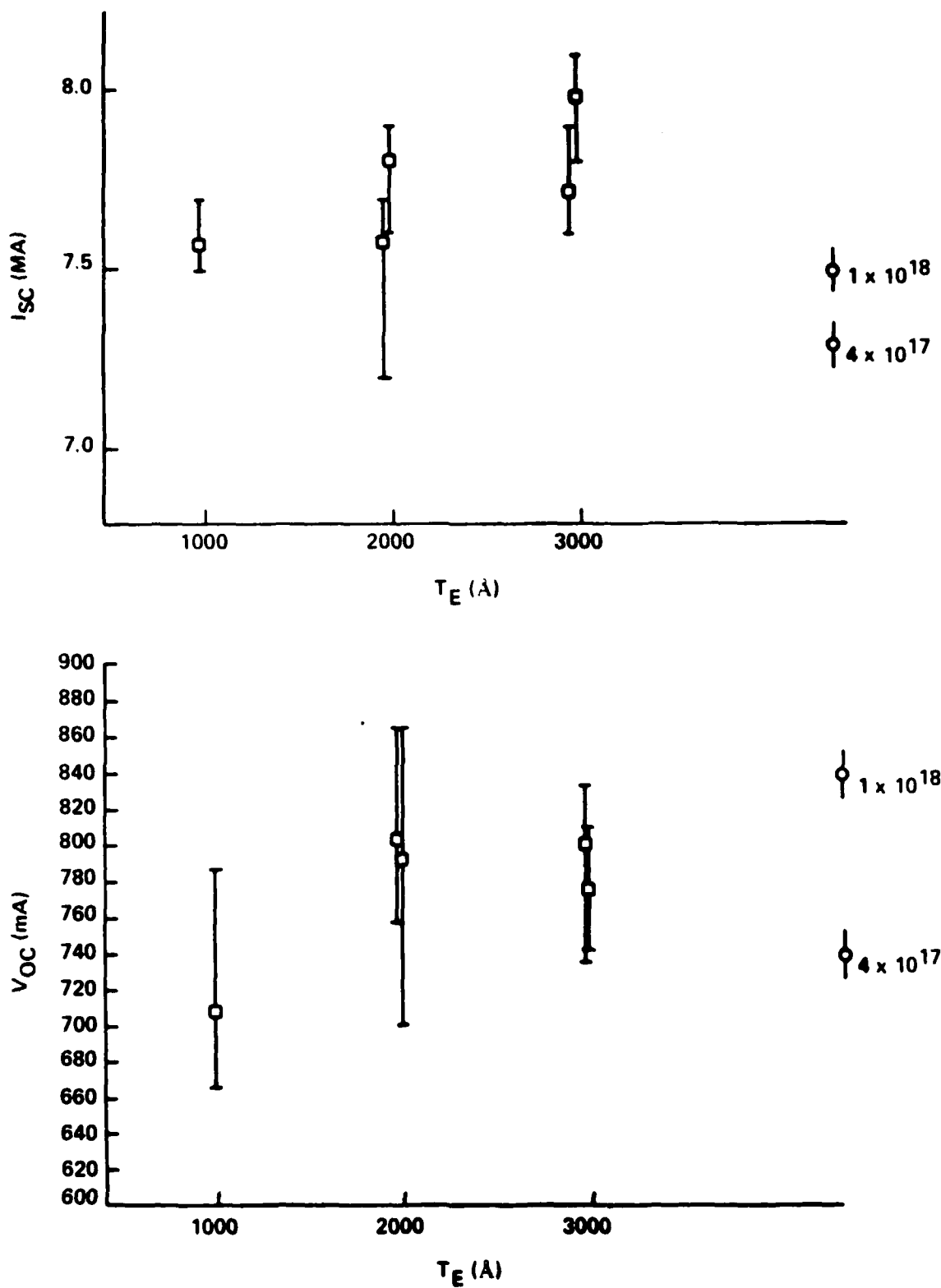


Fig. 17. Average and range of V_{oc} and I_{sc} from cells proposed from samples 30M-372, -388, -371, -373 and -370 (Figs. 12-16).

In the case of n-on-p cells, six growths were carried out to determine the effects of emitter thickness, window thickness, and base doping on the spectral response and I-V characteristics. The relevant parameters are shown in Table 4. Because of a problem in contacting the n-type material on this particular fabrication run, several of the cells have Schottky-like contacts, and the spectral responses and I-V characteristics reflect this fact. The data are displayed in Figs. 18 to 23. Despite the contacting difficulties, three general trends are apparent. First, the thinner window layers produce better spectral response in the UV region of the spectrum, an important feature for an AMO cell. Further work with n-on-p cells, described below, showed the optimum window thickness to be 400 Å. Second, the response is little affected by emitter thickness, indicating that in the range studied the emitter thickness is a forgiving parameter. Finally, lower base dopings, $p \approx 1 \times 10^{17} \text{ cm}^{-3}$, still enhance the red (near-gap) response, as is the case also with p-on-n cells.

TABLE 4: Growth Parameters of n-on-p Cells

<u>Run Number</u>	<u>Emitter Thickness</u>	<u>Window Thickness</u>	<u>Base Doping (cm^{-3})</u> <u>(p-type)</u>
30M402	400	2500	1×10^{17}
30M400	400	2500	5×10^{17}
30M399	400	2500	1×10^{18}
30M404	800	1500	5×10^{17}
30M405	800	1500	1×10^{18}
30M403	800	2500	1×10^{17}

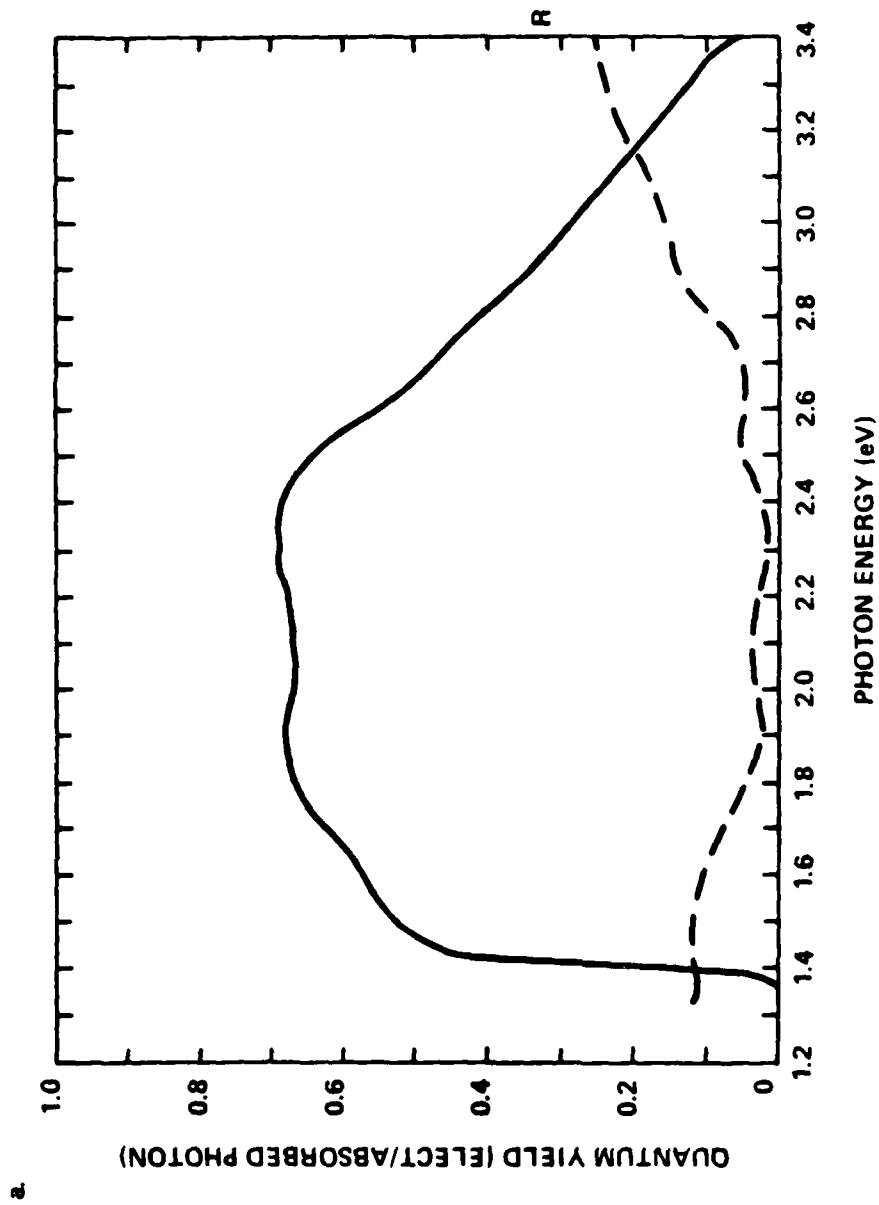


Fig. 18a. Spectral response of an n-on-p GaAs cell (30M-402); emitter thickness 400 Å, window thickness 2500 Å, base doping $1 \times 10^{17} \text{ cm}^{-3}$.

B.

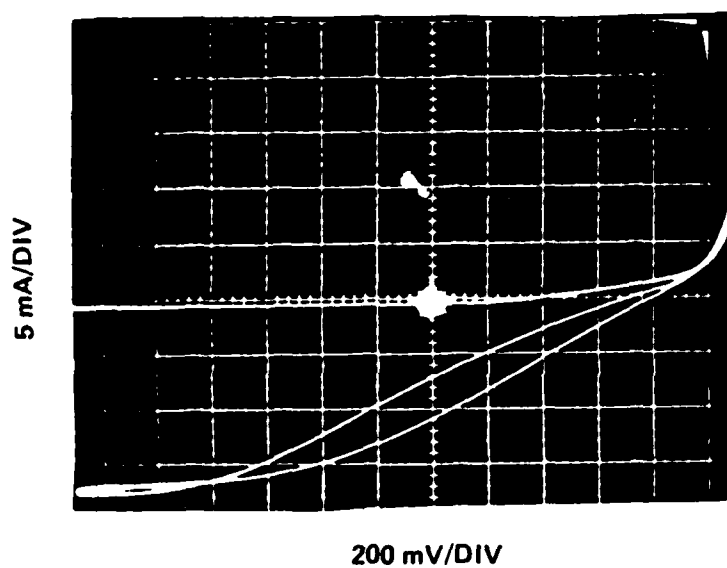


Fig. 18b. I-V characteristic (in dark and under illumination) of the cell in Fig. 18a.

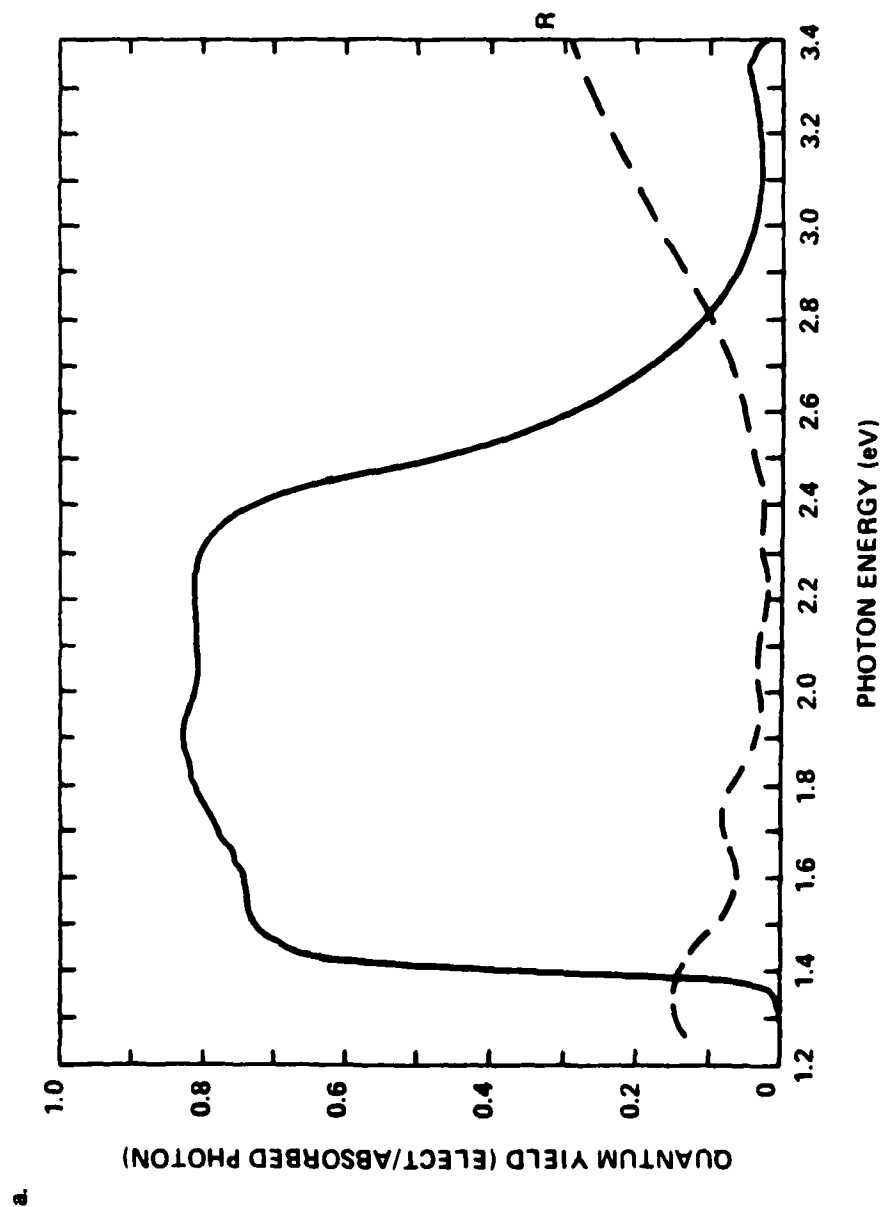


Fig. 19a. Spectral response of an n-on-p GaAs cell (30M-400): emitter thickness 400 Å, window thickness 2500 Å, base doping $5 \times 10^{17} \text{ cm}^{-3}$.

B.

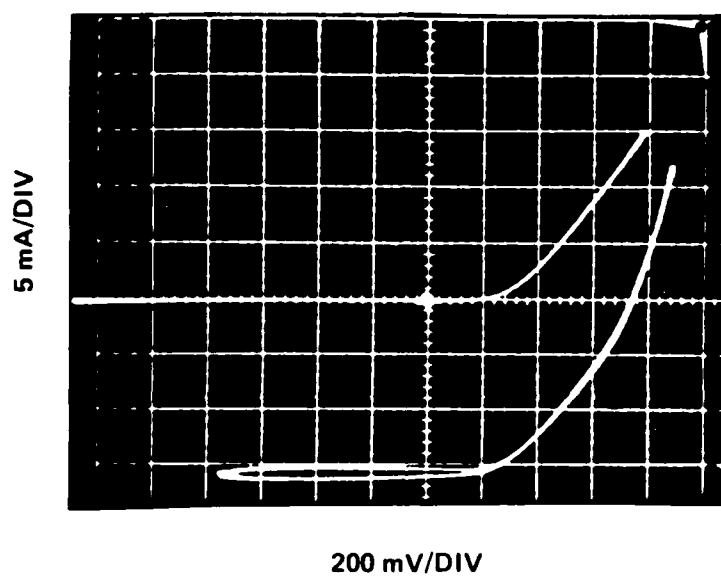


Fig. 19b. I-V characteristic (in dark and under illumination) of the cell in Fig. 19a.

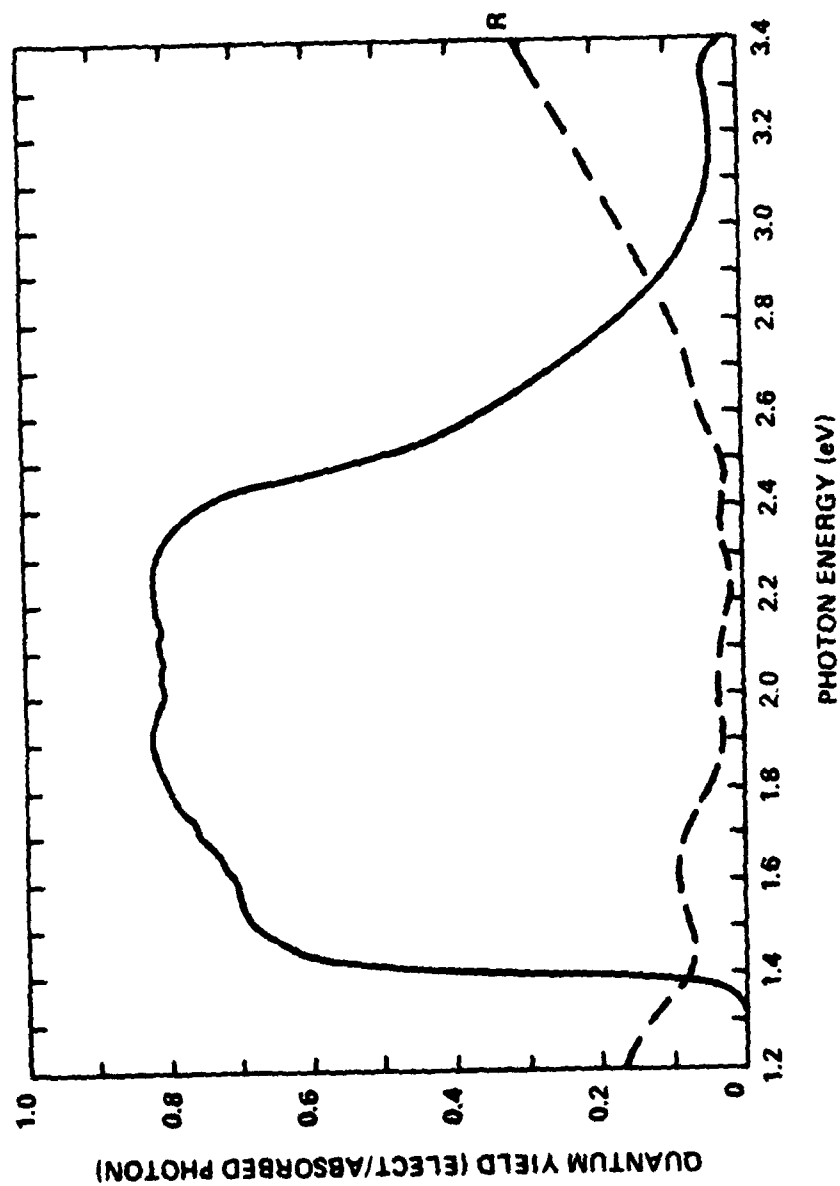


Fig. 20a. Spectral response of an n-on-p GaAs cell (30M-399): emitter thickness 400 Å, window thickness 2500 Å, base doping $1 \times 10^{18} \text{ cm}^{-3}$.

B.

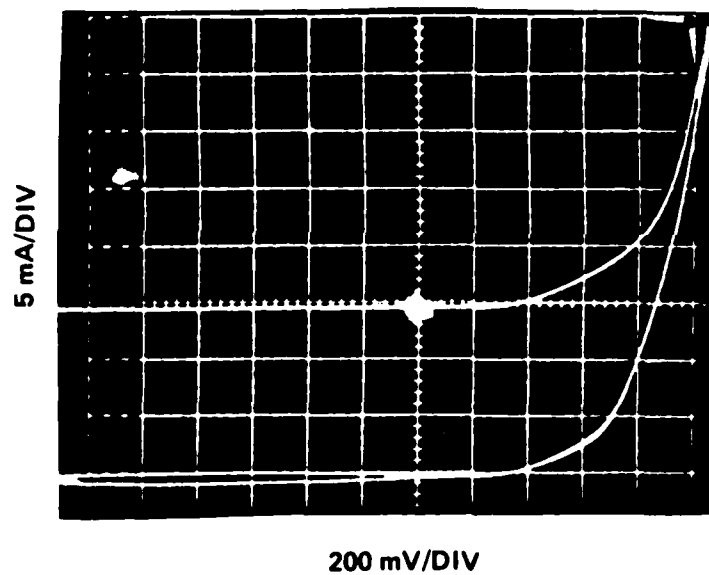


Fig. 20b. I-V characteristic (in dark and under illumination) of cell in Fig. 20a.

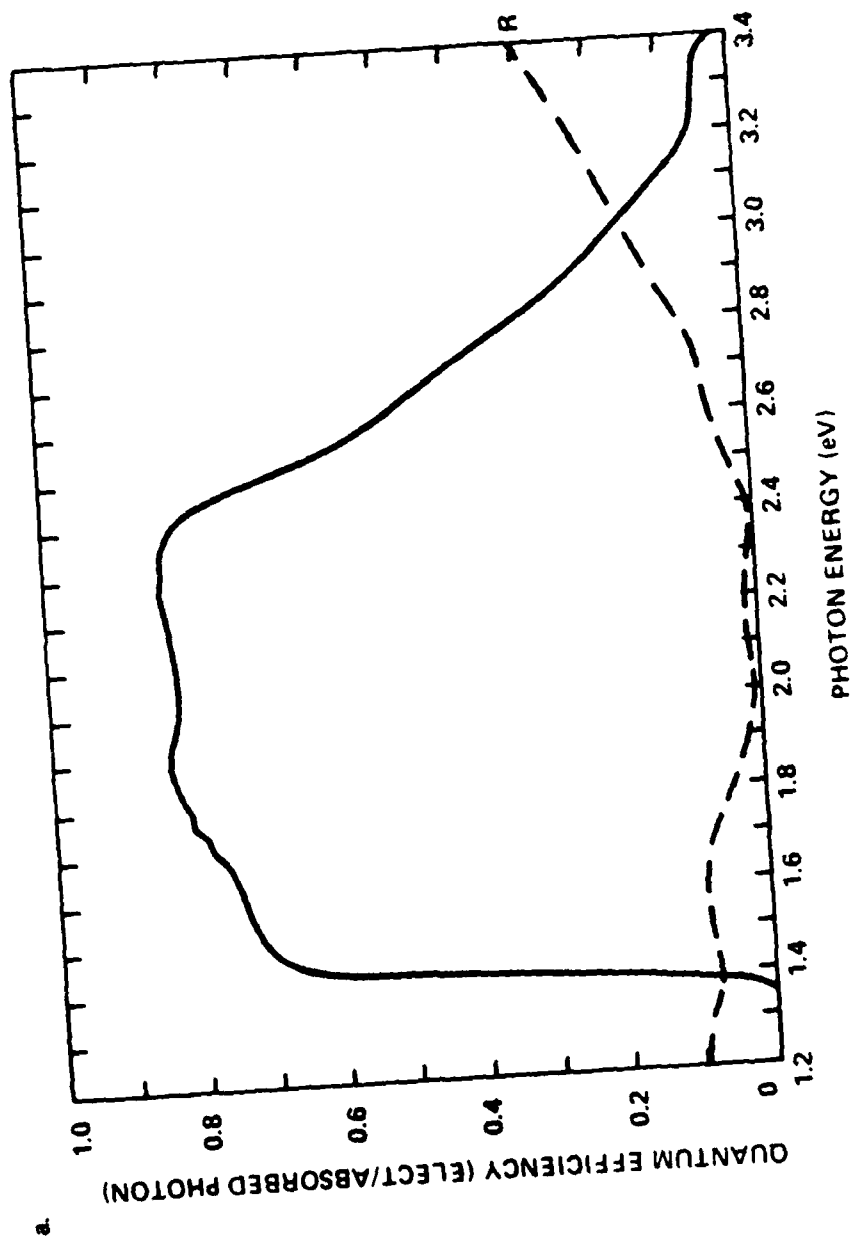


Fig. 21a. Spectral response of an n-on-p GaAs cell (30M-404); emitter thickness 800 Å, window thickness 1500 Å, base doping $5 \times 10^{17} \text{ cm}^{-3}$.

B.

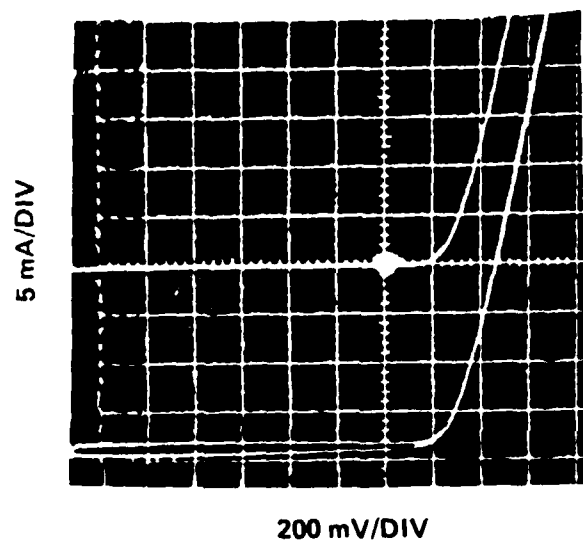


Fig. 21b. I-V characteristic (in dark and under illumination) of cell in Fig. 21a.

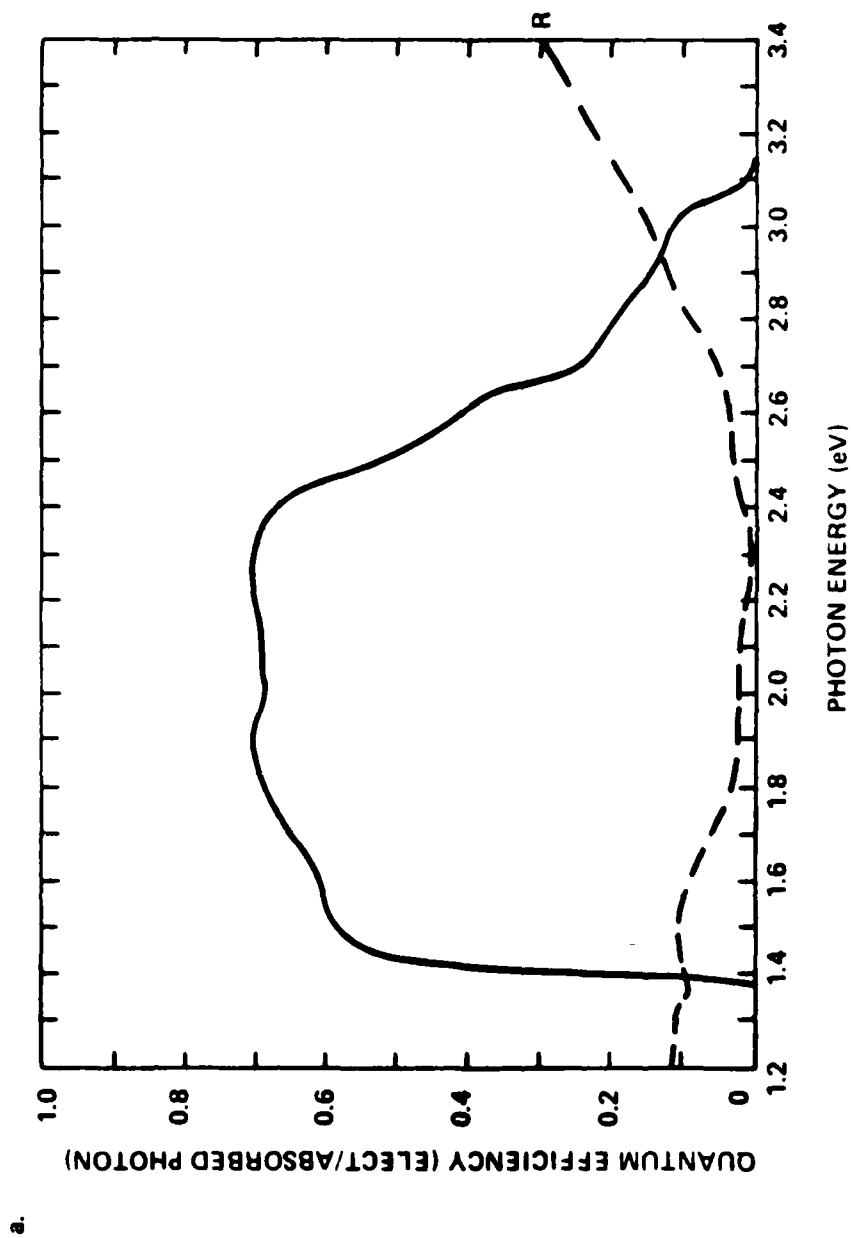


Fig. 22a. Spectral response of an n-on-p GaAs cell (30M-405): emitter thickness 800 Å, window thickness 1500 Å, base doping $1 \times 10^{18} \text{ cm}^{-3}$.

B.

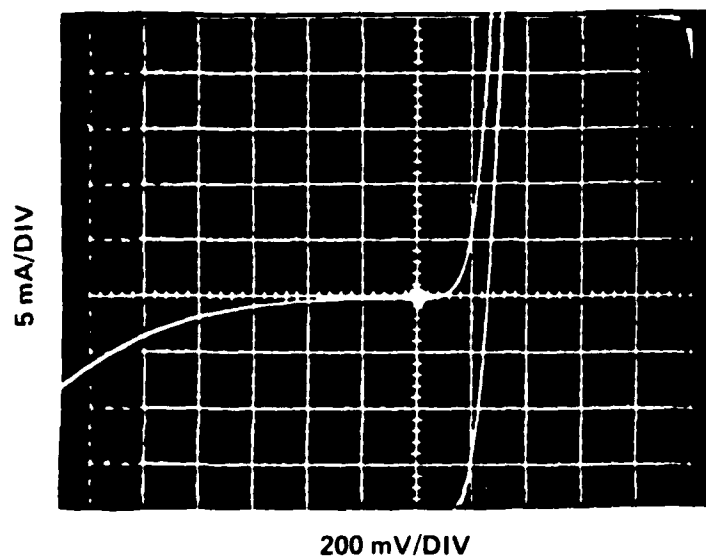


Fig. 22b. I-V characteristic (in dark and under illumination) of cell in Fig. 22a.

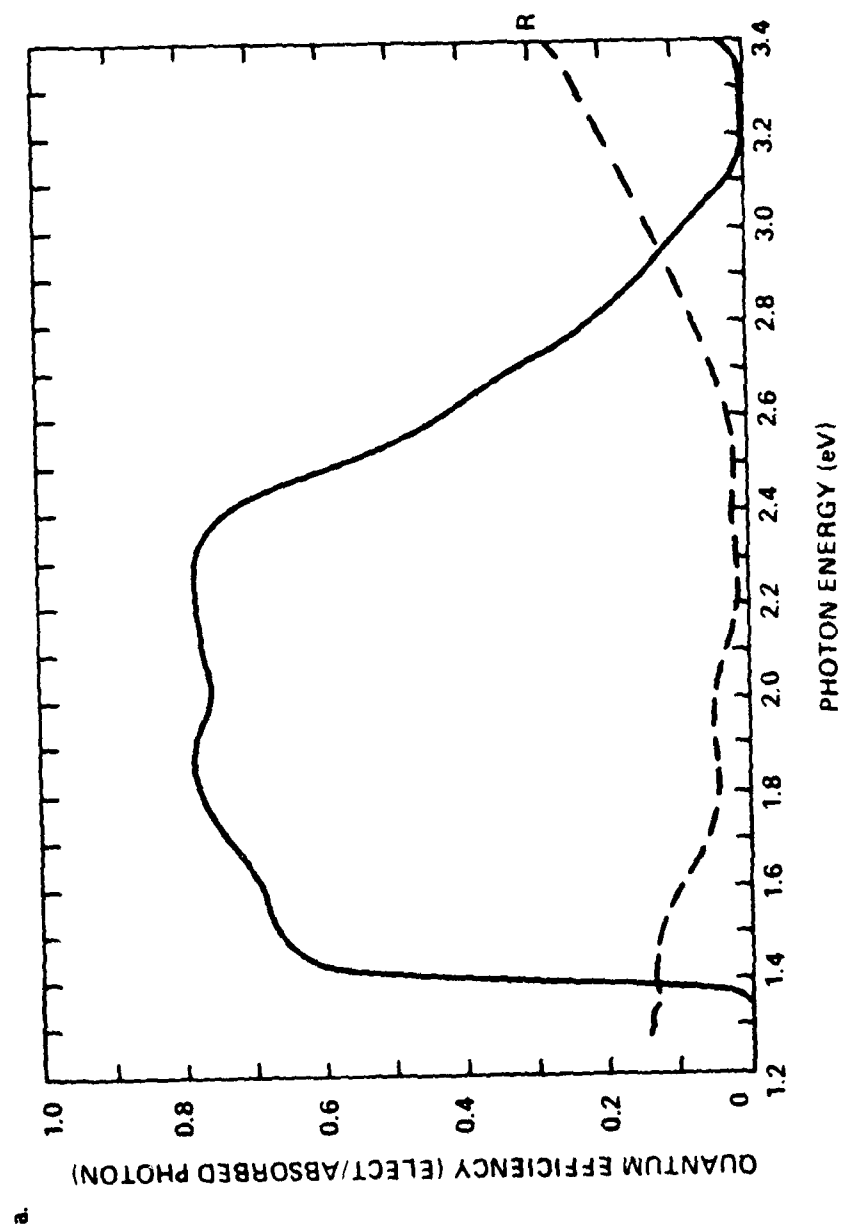


Fig. 23a. Spectral response of an n-on-p GaAs cell (30M-403): emitter thickness 800 Å, window thickness 2500 Å, base doping $1 \times 10^{17} \text{ cm}^{-3}$.

B.

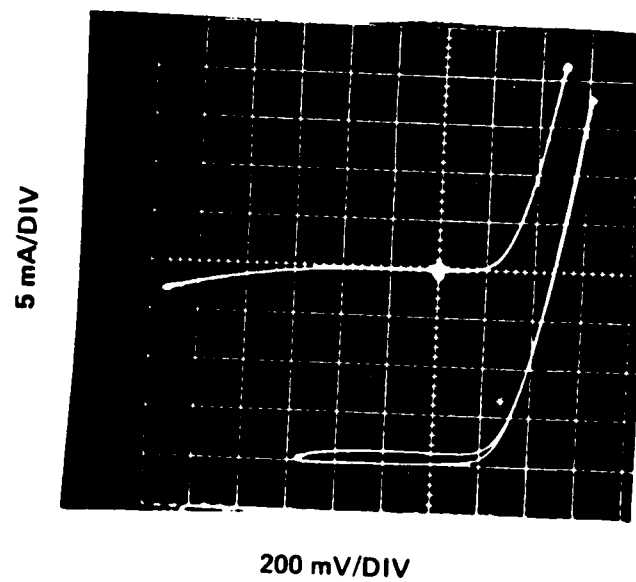


Fig. 23b. I-V characteristic (in dark and under illumination) of cell in Fig. 23a.

A final iteration of n-on-p cell growths was performed, which led to very high spectral responses. The contact problems were resolved by switching to Pd-Au grid metallization. A series of three cells was grown first to recheck the Se doping level in the emitter, and $n = 5 \times 10^{17} \text{ cm}^{-3}$ is optimum. Another series of growths done to finally optimize the spectral response of n-on-p cells produced the response shown in Figs. 24 and 25. The structure of that wafer is, starting at the substrate:

Back field	$\text{Al}_{0.15}\text{Ga}_{0.85}\text{As:Zn}$	$p \sim 10^{18} \text{ cm}^{-3}$	0.2 μm
Base	GaAs:Zn	$p = 5 \times 10^{17}$	2.0 μm
Emitter	GaAs:Se	$n = 2 \times 10^{17}$	0.2 μm
Window	Al_0		
Window	$\text{Al}_{0.80}\text{Ga}_{0.20}\text{As:Se}$	$n = 10^{18}$	400 \AA
Cap	GaAs:Se	$n = 8 \times 10^{18}$	0.2 μm

The differences between the responses shown in Figs. 24 and 25 are attributed to growth-to-growth variations. The investigation was extended one step further to study the effects of growth temperature on spectral response. The usual growth temperature is 730°C; a lowered temperature, 650°C, is desirable, however, because larger uniform areas ($2 \times 4 \text{ in}^2$) are possible. Figure 26 shows the spectral response of the identical structure grown at 650°C. By comparison to Fig. 27, it can be seen that the response is equivalent to the sample grown at the higher temperature.

Both n-on-p and p-on-n cell structures have been developed which are suitable for AMO operation. There were some difficulties encountered while achieving the more desirable n-on-p configuration, mainly in contact formation, but performance is comparable to the best of the samples of the opposite polarity, at least in terms of internal quantum efficiency.

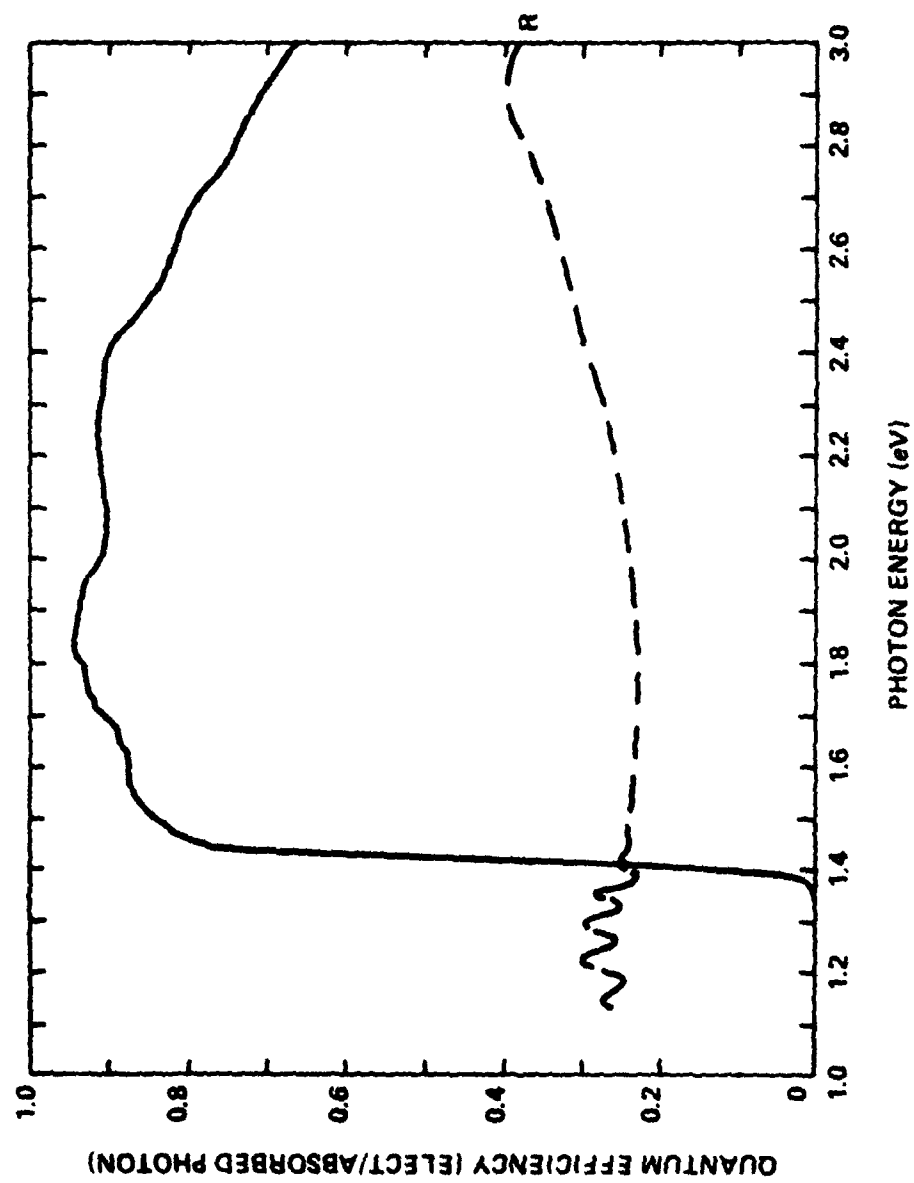


Fig. 24. Final optimization of the spectral response of a GaAs n-on-p cell grown at 730°C.

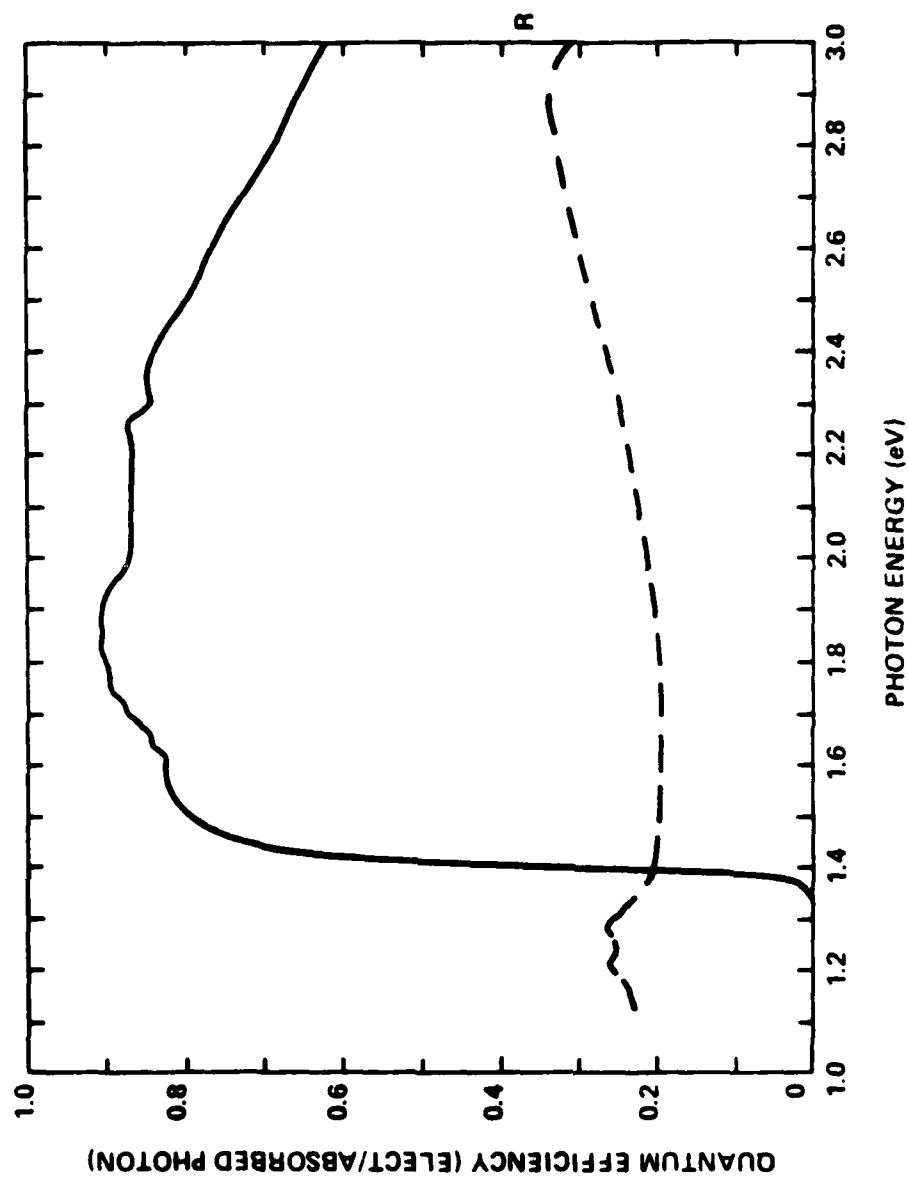


Fig. 25. Final optimization of the spectral response of a GaAs n-on-p cell grown at 730°C. This is a reproducibility check upon the cell of

Fig. 24 and illustrates the magnitude of run-to-run variation.

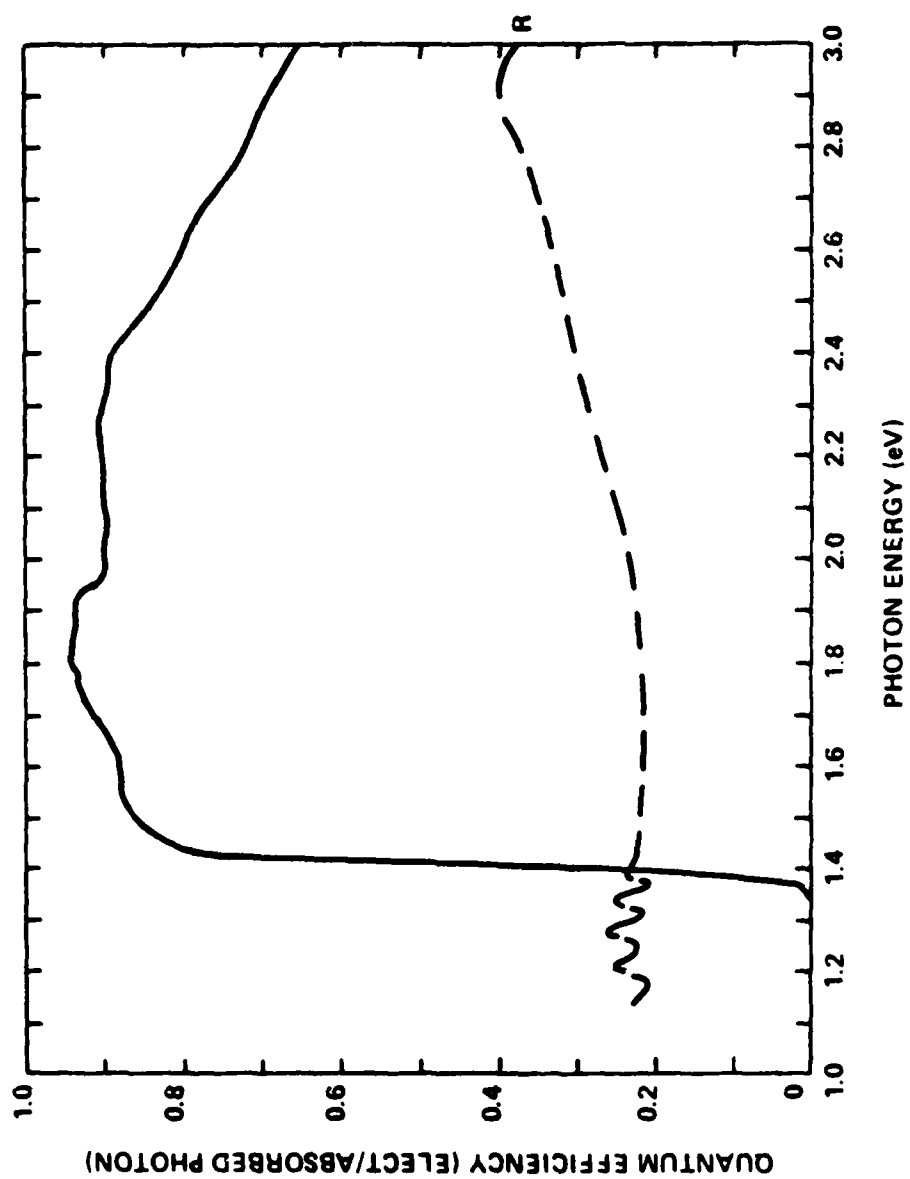


Fig. 26. Final optimization of the spectral response of a GaAs n-on-p cell grown at 650 C.

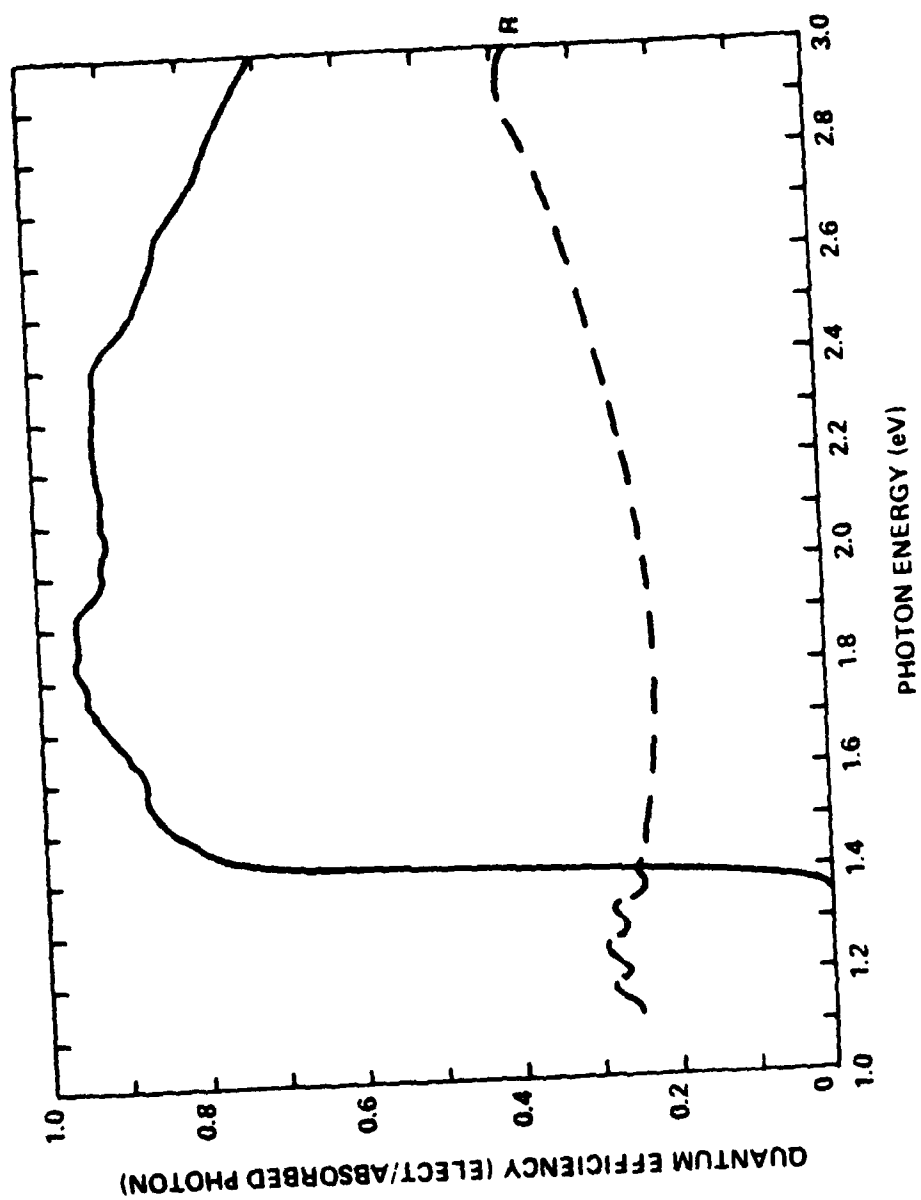


Fig. 27. Final optimization of the spectral response of a GaAs n-on-p cell grown at 730 C.

3. GLASS BONDING AND CELL THINNING PROCESSES

The project goals include a power-to-weight ratio of 550 w/kg with no cover glass a weight of 0.3 grams/ $2 \times 2 \text{ cm}^2$ heterojunction cell. To reach these goals, we have found that it is necessary to remove the GaAs substrate upon which the epitaxial layers of the solar cell are grown.

This thinning process removes approximately 15 mils of GaAs substrate, leaving 6-10 microns of epitaxial material. The resulting epitaxial thickness depends upon the actual cell structure which has been chosen to give the highest efficiency.

The weight of the removed 15 mils of GaAs is 0.81 grams. Thus it is evident that without the substrate removal, the project goal of 0.3 grams could not be met. The remaining 6-10 microns of GaAs weighs 0.013 to 0.021 grams. Assuming a project goal of 18% efficiency, the power-to-weight ratio is then 1869 w/kg for the cell, well above the project goals.

The chosen cover glass is Corning 0211. This glass is readily available in sheets of different areas and also in thicknesses varying from 130 to 250 microns. The weight of a 2-cm x 2.5-cm x 150-micron sheet is 0.19 grams. Thus there will be approximately 0.1 grams available for metallization, interconnects and epoxy before reaching the project goal of 0.3g/finished 2-cm x 2-cm cell.

The results of the thinning experiments have been excellent. Four wafers of over $1 \times 2 \text{ cm}^2$ area each were grown as test samples for the substrate thinning process. The structures consist of a GaAs buffer layer, an $\text{Al}_{0.80}\text{Ga}_{0.20}\text{As}$ stop-etch layer, an $\text{Al}_{0.15}\text{Ga}_{0.85}\text{As}$ base and emitter, an $\text{Al}_{0.90}\text{Ga}_{0.10}\text{As}$ window and a GaAs cap. The total cell thickness is 6 μm . The $\text{Al}_{0.15}\text{Ga}_{0.85}\text{As}$ active layer composition was chosen over GaAs because it is more difficult to grow pinhole-free, and therefore

serves as a more rigorous test. Three wafers were prepared for growth using a technique developed elsewhere in Varian as part of a pilot production program. The fourth wafer was prepared using the previously-used technique. All growths were identical. The three samples grown using the new preparation had essentially zero voids or pinholes; the fourth had the usual high density of voids.

The thinning process, documented in Appendix A, was used to thin these wafers. In summary, the thinning was accomplished by first mechanically lapping with 3- μ m alumina in 10% clorox solution down to 5-mil thickness. A selective etch (95 H_2O_2 :5 NH_3OH) was used to remove the remaining substrate and buffer layers to the stop-etch layer. The stop-etch was removed with buffered oxide etch (BOE). A previous problem has been the persistence of a residue after the BOE etch. It is thought that this residue is aluminum fluoride which is soluble in boiling H_2O . Immersion of the test samples in boiling H_2O does indeed remove most of the residue, although related compounds may not be soluble.

The three samples prepared with the new method had no visible voids over a cumulative area of 6 cm^2 . In contrast, the control sample prepared by the old method had some 15 voids in an area of 2.6 cm^2 . Thus, there is now a repeatable technique for producing voidless epilayers. The problem of voids had been the single most vexing hindrance in obtaining an epilayer-thinned cell.

The thinned bonded layers were profiled using a Dektak II. One result of the thinning was a lip on the edge of the thinned sample. Figure 28 shows a 2.5-mm wide by about 25- μ m high edge lip on the 10- μ m thick sample. The defect shown is due to an air bubble caught between the sample and the glass. Neither of these present any problems in the fabrication of thinned cells. The PV cells themselves will be further from the edges of the wafers than 2.5 mm, and the air bubble does not present a current leakage problem.

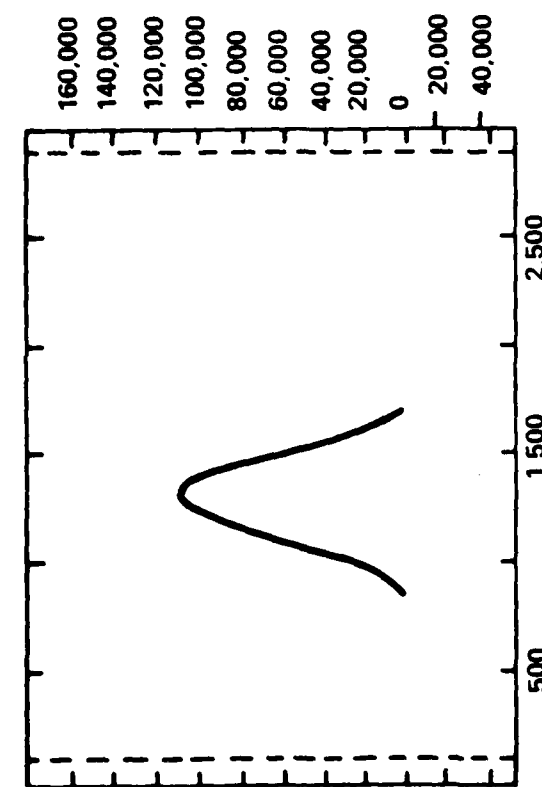
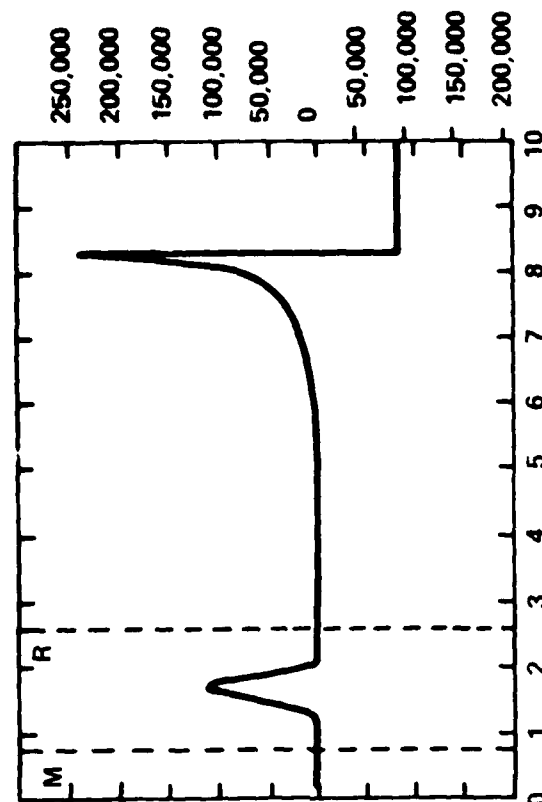
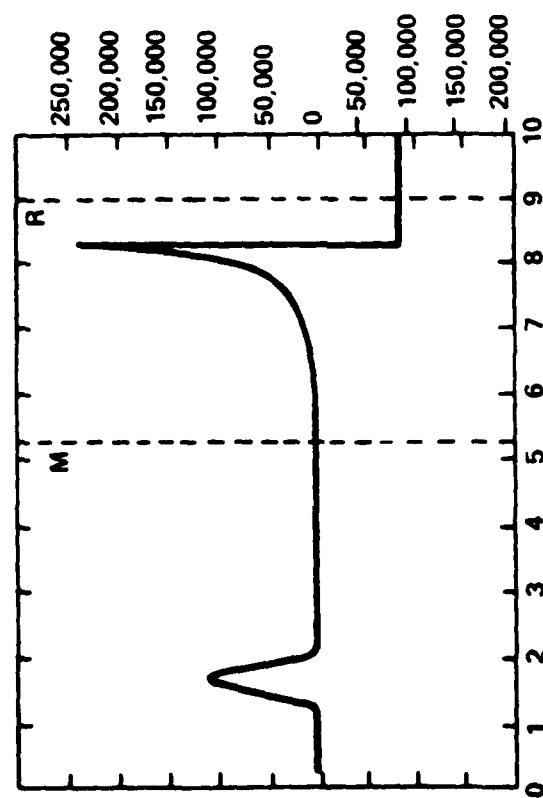
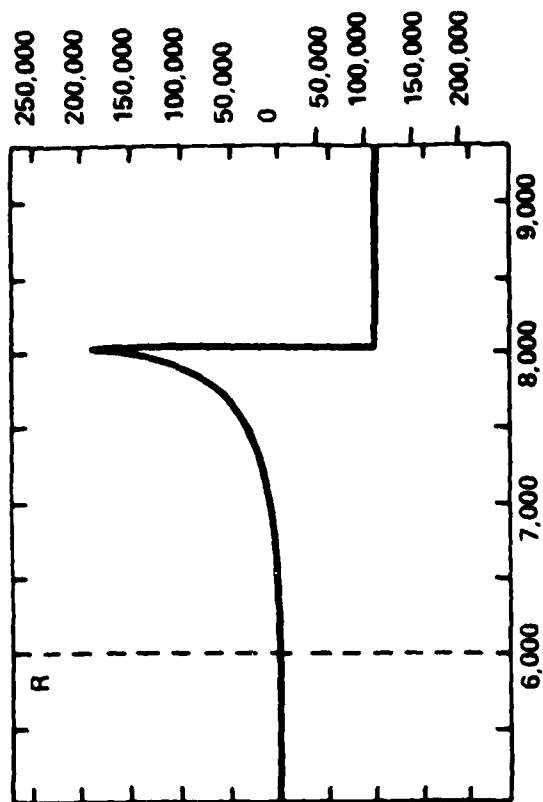


Fig. 28 Dektak II profiles of thinned bonded wafers, illustrating a lip on the sample edge after thinning. The lip is due to a trapped air bubble. The height in Å (y coordinate) is plotted as a function of horizontal distance in mm or μm (x coordinate).

4. OTHER TASKS

a. Thin Cell Fabrication

The contract was terminated before work was performed under this task.

b. Welded Contacts

The contract was terminated before this task was scheduled to begin.

c. Cost Study

The contract was terminated before this task was to begin.

d. Testing

No complete cells were fabricated, and thus no performance tests were run.

e. Cell Deliveries

The program was terminated prior to the commencement of cell fabrication, so no deliveries are possible.

APPENDIX A: THINNING PROCESS

<u>Purpose:</u>	To mount MOCVD solar cell onto glass cover and the remove substrate from epitaxially-grown active region of ~0.6-micron thickness.	
<u>Equipment:</u>	Analytical balance 6000 RPM wafer spinner 120°C and 150°C N ₂ ovens lapping machine mounting press	
<u>Chemicals:</u>	TCE Sylgard primer Sylgard 182 resin Sylgard 182 curing agent Bleach BOE	Acetone IPA mounting wax 3-micron microgrit 0.3-micron micropolish McGeam CB 165 HF silicon stripper deionized water
<u>Tools:</u>	2" x 3" glass slide glass puck Q-tips air brush teflon tweezers SS spatula	SS tweezers teflon holders politex supreme pad scalpel wire brush

STEP BY STEP:

A. Bonding Cell to Corning 0211 Glass

1. Acetone, IPA clean 2x3-inch glass slide for mixing Sylgard 182 epoxy.
2. Heat slide @ 120°C for 20 min. in oven, cool to room temperature covered by Petri dish.
3. Weigh out Sylgard 182, resin, curing agent, 10:1 on analytical balance. Use about 0.3-0.5 g of resin; ratio should be $\pm 5\%$.

4. Mix well with clean SS spatula and place under a Petri dish cover. Let stand for ≥ 30 min. to let air bubbles escape.
5. Spin solvent clean solar cell and cover glass with TCE, acetone, and IPA.
6. Bake dry @ 120°C for 15 minutes.
7. Spin Sylgard primer onto the glass and the top of the solar cell @ 6000 RPM @ 20 sec.
8. Cover both and let dry for 30 min., but no longer than 45 min., at room temperature.
9. Place cell, top up, on clean Teflon holder and apply small amount of Sylgard to the top of the cell.
10. Place glass on the cell, primed side down, careful not to trap air bubbles. Press on glass to spread out Sylgard and remove bubbles.
11. Place in mounting press and cure in N_2 oven @ 150°C for 1 hour.

B. Thinning Preparation

1. When cool, remove from press and mount on glass puck with mounting wax, glass toward puck. Make sure cell is flat on puck.
2. Remove excess wax with TCE and Q-tips.
3. Place cell into Petri dish with McGeam CB-165 HF silicon stripper for 3 minutes.
4. Remove excess Sylgard with scalpel, wire brush and Q-tips.
5. Clean puck-mounted wafer & glass with TCE and Q-tip.

C. Thinning Mounted Cells

1. Measure thickness of mounted cell -- should be about 15 mil.
2. Mechanically lap mounted cell down to about 5 mil using Geos Corp. 3-micron microgrit, alconox and water on the lapping machine.
3. Rinse with DI water.
4. Clean puck and cell with TCE & Q-tip to remove remnants of 3-micron grit.
5. Polish using Buehler 0.3-micron micropolish and clorox bleach or Polatex supreme pad until GaAs substrate surface is mirrorlike.
6. Remove wafer and glass from puck and remove excess wax with 2 hot TCE dips, blow dry.
7. Place mounted cell 30° to vertical in stop etch. $H_2O_2; NH_4OH$, 95:5 -- use teflon tweezers, rotate cell 90° every 10 minutes until etch stops at $Al_{0.8}Ga_{0.2}As$ layer.
8. Rinse in DI water.

9. Remove $\text{Al}_{0.8}\text{Ga}_{0.2}\text{As}$ layer by 1 minute in BOE.
10. Rinse in DI water.
11. Place in boiling DI for 5 minutes to remove residue.
12. Rinse in DI water, blow dry.

THINNING PROCESS -- NOTES

1. Mounting -- Sylgard

Bonding is a critical point in the process. If the glue is too thick, the wafer will be more susceptible to mechanical damage. If the surfaces are not cleaned properly, the cell will delaminate. Particles trapped between the cell and glass may puncture the cell when it is thinned or may cause the etch to break through the stop-etch and cause a pinhole. Any particle bigger than 3 microns is significant. Excessive pressure at bonding causes stresses in the cell which cause it to fracture when lapped.

The Sylgard is very pliant, transparent to light of 0.350-1.1 microns wavelength, and impervious to almost all aqueous solutions. Acetone and TCE cause it to swell, but have no apparent lasting effects. IPA and methanol have the same effect, but to a lesser degree. McGeam silicon stripper, CB-105F, makes it easy to remove but does not just dissolve it. It must be soaked and mechanically removed; there always seems to be a residue left which makes the glass hydrophobic. Thermal tests have showed that it begins to outgas at 320°C, and "smokes" at 350°C; but if it is enclosed by glass on both sides, it can be heated up to 375°C for 2 minutes without significant degradation.

Sylgard is very sensitive to other epoxies. Allowing even a part of the resin to contact an epoxy can prevent the whole quantity from curing properly. It is a good idea to take some of the resin and cure it to be sure it is a good batch.

2. Thinning

The wafer is lapped and polished for these reasons:

- a. to remove all traces of metal and Sylgard,
- b. to even up the surface and remove surface damage,
- c. to leave a chemically-clean, oxide-free surface, and
- d. to remove bulk GaAs quicker than the etch so that the etch reaches the stop-etch layer of $\text{Al}_{0.8}\text{Ga}_{0.2}\text{As}$ with greater uniformity.

Perhaps the polishing could be skipped in favor of a 4:1:1 etch.

The 95:5 etch is very sensitive to surface preparation, and any "crust" that forms on the surface is next to impossible to remove. It is content to etch on the (100) plane, but if disturbed, will begin to etch out the (111) planes and the surface will appear to have a sheen that catches the light at a certain angle. Fresh etch and a separate beaker must be used for each wafer.

Metal ions destroy the bath -- this is the reason for the teflon tweezer. The NH_4OH must come in plastic bottles, for the glass bottles leach out the metal (Na) ions.

When the wafer is put into the etch, it must be:

- a. dry,
- b. oxide free, and
- c. clean of organics.

Water on the surface tends to create an oxide layer, and this grows a crust which creates a ridge (similar to the organics). Bubbles must be brushed away from the wafer, since they also cause ridges; but they can be allowed to remain on the very edge since the etch is faster there anyway. The wafer must sit in the etch face up at an angle of 30-45° w.r.t. the vertical. Flowing down the surface in a sheet, the reaction by-products from above affect the operation of the etch below; in fact, the etch rate at the top is about twice that at the bottom on a 1" wafer. Thus the wafer must be inverted during the etch.

At the stop-etch layer (80-90% Al), the etch slows drastically but does continue. Depending on agitation, presence of unremoved GaAs and other conditions, the etch rate of the AlGaAs varies between 10 and 100 Å/min. This is why it is important to obtain an even etch -- so that the etch-stop will not be penetrated while the other part finishes etching. (Also, there is the problem of etching in from the edges of the wafer.) If black wax is put

onto the surface to mask finished areas while others etch, sometimes the stop-etch (right at the edge of the wax) will etch away for no apparent reason.

The 5-minute boiling water is to remove remnants of aluminum fluoride left as a residue after the $\text{Al}_{0.8}\text{Ga}_{0.2}\text{As}$ is etched off with BOE.

DATE
FILME